Unbiased Proteomics, Histochemistry, and Mitochondrial DNA Copy Number Reveal Better Mitochondrial Health in Muscle of High Functioning Octogenarians

Ceereena Ubaida-Mohien PhD[1], Sally Spendiff PhD[2], Alexey Lyashkov PhD[1], Ruin Moaddel PhD[1], Norah J. MacMillan MD[3], Marie-Eve Filion MSc[3], Jose A. Morais MD[3], Tanja Taivassalo PhD[4], Luigi Ferrucci MD PhD[1]*, Russell T. Hepple PhD[4,5]*

[1]Intramural Research Program, National Institute on Aging, National Institutes of Health, Baltimore, MD, USA; [2]Children's Hospital of Eastern Ontario Research Institute, 401 Smyth Rd, Ottawa, CANADA; [3]Research Institute of the McGill University Health Centre, McGill University, Qc, CANADA; [4]Department of Physical Therapy, University of Florida, FL, USA; [5]Department of Physiology and Functional Genomics, University of Florida, FL, USA

*Luigi Ferrucci and Russell T. Hepple share senior authorship.

Correspondence:

Luigi Ferrucci

Translational Gerentology Branch, National Institute on Aging, National Institutes of Health, Baltimore, MD. Ph) 410-558-8110, Email: ferruccilu@grc.nia.nih.gov

Russell T. Hepple

Department of Physical Therapy, University of Florida,1225 Center Drive, Gainesville, FL, USA 32608. Ph) 352-294-8703, Email: rthepple@ufl.edu

DATA AVAILABILITY. The mass spectrometry proteomics data have been deposited to the MassIVE with the dataset identifier MSV000086195 (ftp://MSV000086195@massive.ucsd.edu), reviewer user name (MSV000086195_reviewer).

Funding: Funding for this study was provided by operating grants from the Canadian Institutes of Health Research (MOP 84408 to TT and MOP 125986 to RTH). Supported in part by the Intramural Research Program of the National Institute on Aging, NIH, Baltimore, MD, United States.

Conflict of Interest Disclosure. The authors have no conflicts of interest to disclose.

Ethics Approval and Patient Consent. Human subjects research was done with prior approval from the Institutional Review Board of the Faculty of Medicine at McGill University (A08-M66-12B) and according to the Declaration of Helsinki. All subjects provided written informed consent.

Abstract

Background: Master athletes prove that preserving a high level of physical function up to very late in life is possible, but the mechanisms responsible for their high function remain unclear.

Methods: We performed muscle biopsies in 15 octogenarian world class track and field masters athletes (MA) and 14 non-athlete age/sex-matched controls (NA) to provide insights into mechanisms for preserving function in advanced age. Muscle samples were assessed for respiratory compromised fibers, mtDNA copy number, and proteomics by liquid-chromatography mass spectrometry.

Results: Most of the ~800 differentially represented proteins in MA versus NA pertained to mitochondria structure/function such as electron transport capacity (ETC), cristae formation, mitochondrial biogenesis, and mtDNA-encoded proteins. In contrast, proteins from the spliceosome complex and nuclear pore were downregulated in MA. Consistent with proteomics data, MA had fewer respiratory compromised fibers, higher mtDNA copy number, and an increased protein ratio of the cristae-bound ETC subunits relative to the outer mitochondrial membrane protein voltage dependent anion channel. There was a substantial overlap of proteins overrepresented in MA versus NA with proteins that decline with aging and which are higher in physically active than sedentary individuals. However, we also found 176 proteins related to mitochondria that are uniquely differentially expressed in MA.

Discussion: We conclude that high function in advanced age is associated with preserving mitochondrial structure/function proteins, with under-representation of proteins involved in the spliceosome and nuclear pore complex. Whereas many of these differences in MA appear related to their physical activity habits, others may reflect unique biological (e.g., gene, environment) mechanisms that preserve muscle integrity and function with aging.

Keywords: Master Athletes, non athletes, proteomics, skeletal muscle, mitochondria, spliceosome, aging, mass spectrometry, nuclear pore, octogenarians, physical activity, exercise

1 INTRODUCTION

The aging process is associated with profound changes in body composition that includes a substantial decline of muscle mass and a disproportionally more severe decline in strength (Goodpaster *et al.*, 2006). Such decline in skeletal muscle mass and strength starts between the third and the fourth decades of life both in men and women, substantially accelerates after the age of 75 years, and in some individuals becomes so severe as to cause mobility loss and frailty (Cawthon *et al.*, 2019). However, there is clear evidence that such "usual" decline of strength and function is not an inescapable consequence of aging. For example, some athletes retain remarkably high physical performance in their eighties and nineties and there have been sporadic mentions of centenarians who compete in marathons (https://www.runnersworld.com/runners-stories/a20812407/whos-the-fastest-centenarian/). The study of these extreme examples provides a unique opportunity to identify mechanisms that in most individuals determine a decline of muscle health with aging, but which are counteracted in highly functioning individuals. For example, we have previously shown highly functioning octogenarian track and field athletes better maintain the number and transmission stability of motor units (Power *et al.*, 2016) and exhibit high muscle fiber reinnervation capacity (Sonjak *et al.*, 2019) compared to healthy octogenarian non-athletes and pre-frail/frail octogenarians, respectively.

Using a discovery, unbiased proteomics approach on skeletal muscle biopsies collected in very healthy individuals aged 20 to 87 years, we previously found that older age was associated with underrepresentation of mitochondrial proteins, especially those associated with oxidative phosphorylation and energy metabolism (Ubaida-Mohien *et al.*, 2019b). Besides, independent of age, 75% of proteins overrepresented in persons who were more physically active in their daily life were mitochondrial proteins across the different sub-localization or function (Ubaida-Mohien *et al.*, 2019a). These data strongly suggest that maintaining mitochondrial function is a key to healthy muscle with aging. However, because both mitochondrial function and physical activity level both decline with aging even in healthy individuals, discriminating their independent effects on muscle health remains problematic. The study of muscle biopsies in highly trained, older individuals compared with age-matched controls should overcome, at least in part, this limitation.

In this study, we used data and biological specimens collected in 15 track and field masters athletes (MA) aged 75 to 93 y (8 females), eight of whom were world record holders in their age

group for at least one event at the time of study, with the remaining individuals ranked in the top 5 world-wide for their respective age and discipline. These individuals are representative of the extreme tail of the distribution of physical fitness in their age group. These master athletes were compared with 14 age- and sex-matched non-athletes recruited from the greater Montreal area (NA; 6 females) to represent healthy independent octogenarian individuals. We compared in these two groups cardiopulmonary fitness (cycle test), isokinetic knee extensor strength, and lower extremity function (time to walk 4m fast, chair stands, stand-up and go fast, balance time). In addition, we used magnetic resonance imaging of the thigh to determine muscle cross-sectional area. We performed in-depth skeletal muscle phenotyping using muscle biopsies collected by Bergstrom needle from the vastus lateralis for an unbiased proteomics analyses, histochemical characterization of proteins involved in oxidative phosphorylation (oxphos) and assessment of mitochondrial DNA (mtDNA) copy number by real time polymerase chain reaction (qPCR). High physical function in octogenarians was associated with overrepresentation of the mitochondrial proteome, underrepresentation of mRNA processing and pre-mRNA splicing, fewer oxphos compromised muscle fibers and higher mtDNA copy number, implicating mitochondrial health in skeletal muscle as a key feature facilitating high physical function in advanced age.

2 RESULTS

2.1 Superior clinical function in master athletes (MA) versus non-athlete controls (NA)

The general characteristics of the 15 MA and 14 NA participants are summarized in Table 1.

Table 1. Characteristics of NA and MA.

		NA (n=14)	MA (n=15)	P-value
Age, Y		80.9 ± 4.5	80.1 ± 4.8	
Sex	Male	7	7	
	Female	7	8	
Body Mass, kg		72.1 ± 11.4	62.2 ± 10.7	0.04
Body Fat, %		36.0 ± 6.6	21.9 ± 5.0	<0.00

Values are means ± SD.

The athletes could generally be subdivided into two groups based upon their preferred competition events. Sprint/Power athletes comprised individuals who competed in multi-sport jumping, throwing, and sprinting events; and individuals who competed in sprint running. Endurance athletes competed in track running and road running distances from 400 m to a full marathon (26.2 miles). An overview of the training and competition history of the MA group is in Table 2. With respect to their training habits, it should be noted that each subject commented that the training load (particularly intensity) varied not only within a competition season but also within a 5 y age bracket (e.g., 75 to 79 y, 80-84 y, etc.). Training typically increased in the months approaching a birthday that would move them up to the next age category to take advantage of being the "youngest" in their new age bracket at international competitions. In addition, regardless of the preferred competition events, all athletes noted a very mixed training regimen consisting of varying amounts of running, cycling, walking, stretching, yoga and strength training. The rationale for selecting athletes from a broad array of athletics disciplines was that we were not interested in the effects of a specific type of exercise training *per se* (e.g., endurance or strength training), but rather in identifying individuals with exceptional physical capabilities regardless of their training. Consistent with this rationale, MA participants had superior function during the assessment of VO_{2max}, peak cycle work rate, time to walk 4 m fast, chair stands, stand up and go, and balance time versus NA (Figure 1 a-f), confirming that they represent high functioning octogenarians.

Table 2. Training and competition history of octogenarian MA.

	n	Age, Y	Training per wk (h)	Years competing
Sprint, Power	8 (4 F)	79.9 ± 6.1	16 ± 3	16.6 ± 6.2
Endurance	7 (4 F)	80.3 ± 3.4	14 ± 5	26.6 ± 9.4

Values are means ± SD.

Figure 1

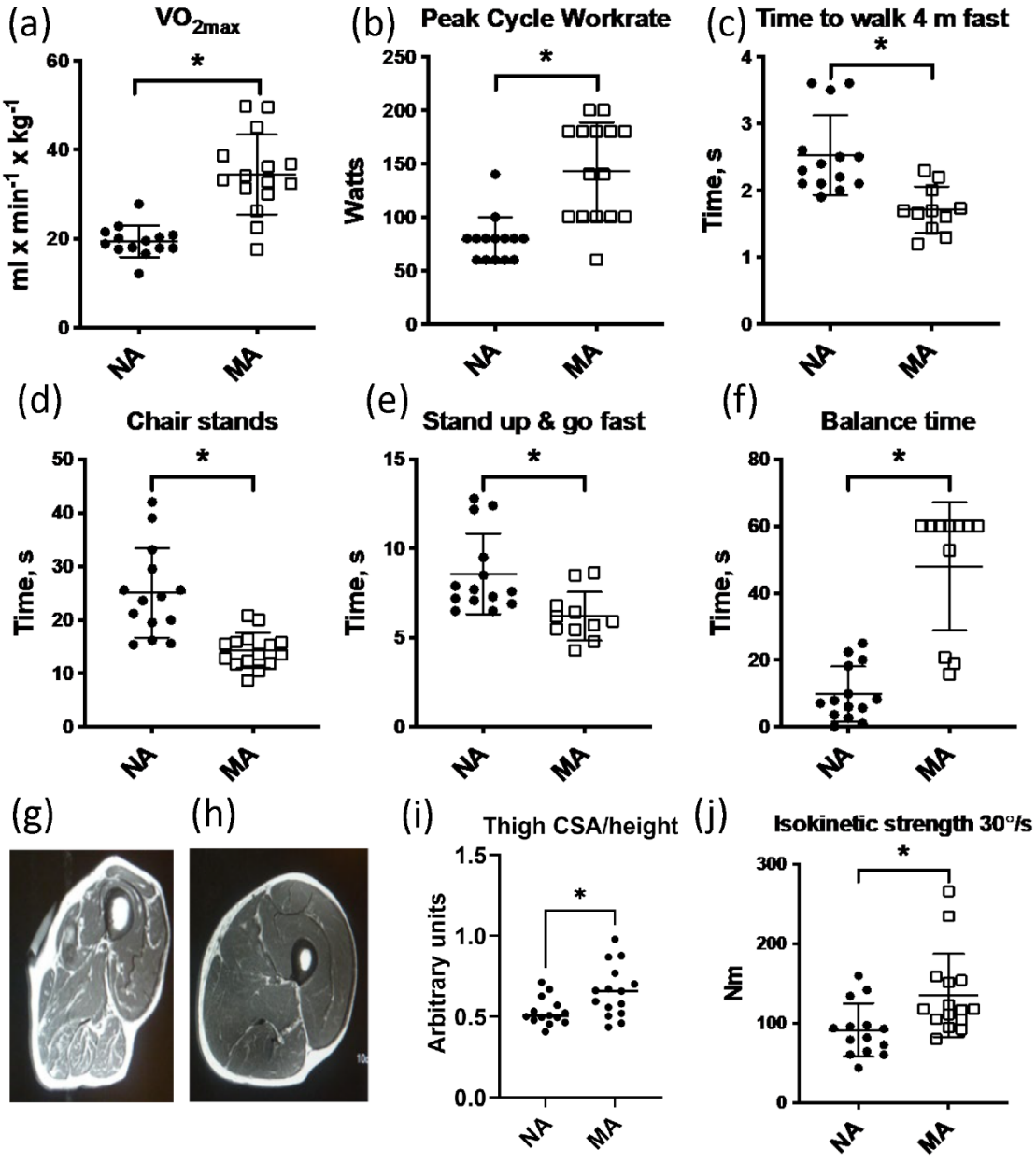

2.2 Greater preservation of muscle mass in octogenarian MA

All MA and NA participants underwent an MRI scan of the mid-thigh region at the same level as the muscle biopsy. Thigh cross sectional image of participant (Figure 1g-h) and MRI cross sectional image of participants were analyzed (Figure 1i). The area of the vastus lateralis muscle (biopsied muscle) was determined for both legs. The estimated muscle cross-sectional area (CSA) of the thigh (normalized by height) was significantly higher in MAs than NA (Figure 1j). Maximal isokinetic strength during knee extension was significantly greater in MA than NA.

To consider the myosin genes that encode muscle mass maintenance and skeletal muscle contraction, we performed a fiber type proportion and fiber size type analysis (type I, type IIa, type IIx, and hybrid) by immunolabeling for the major myosin heavy chain isoforms in MA and NA. This analysis shows very subtle differences that did not reach statistical significance between MA and NA groups (Figure 1-figure supplement 1, panel A). This analysis is corroborated by our proteomics data which also shows very subtle differences in the expression of MYH7 (type 1), MYH2 (type IIa), MYH1 (type 2x), and negligible expression of MYH4 (type IIb) as expected (Figure 1-figure supplement 1, panel B). Indeed, after accounting for the false discovery rate, there were no significant differences in myosin heavy chains between groups. Further to this, there were no significant differences in fiber size by type or in the type I to type II cross-sectional area ratio between MA and NA (Figure 1-figure supplement 1, panels C and D, respectively).

2.3 Quantitative proteomics reveals temporal proteome differences between MA and NA

To understand how skeletal muscle protein composition differs between MA and NA octogenarians, we performed a discovery proteomic analysis of muscle biopsies using LC-MS. We used a 10-plex Tandem Mass Tag (TMT) labeling approach that allows quantification and direct comparison between samples. Analyzing 28 participants, we were able to quantify 6,176 proteins (Figure 2a, Figure 2-figure supplement 1). Of these, 4,178 proteins (68%) were quantifiable across three TMT batches (present in all donors), and 1,998 proteins (18%) were quantifiable in only one TMT batch (present in at least 10 donors). The quantitative protein expression between the TMT batches (Figure 2b) was mostly similar. The list of all proteins quantified from the MA and NA skeletal muscle are reported in Table S1. The Principal Least Square (PLS) dimensionality reduction method used to stratify proteome distribution between MA and NA from 24 donors (Figure 2c) reveals a clear separation between the groups along the PC1 (11.6%) and PC2 (16.7%) axes and PC3 (11.1%) axes.

Of all the 6,176 proteins quantified, 880 were differentially represented between MA and NA (Student's *t*-test, $p<0.05$, FC >1.02 for overrepresented proteins and <0.9 for underrepresented proteins), and of these, 544 proteins were overrepresented and 336 proteins were underrepresented in MA compared to NA (Figure 2d, Table S2a-b). Uniprot cellular localization coverage for these divergently represented proteins is shown in Figure 2e. Of note, 42% of the total 880 significantly altered proteins in octogenarians were mitochondrial proteome, and most of the differentially represented proteins relate to mitochondrial structure or oxidative

178 phosphorylation. This ample coverage of the mitochondrial proteome enables us to explore the
179 modulating role of mitochondria in high functioning octogenarians' muscle metabolism.

Figure 2

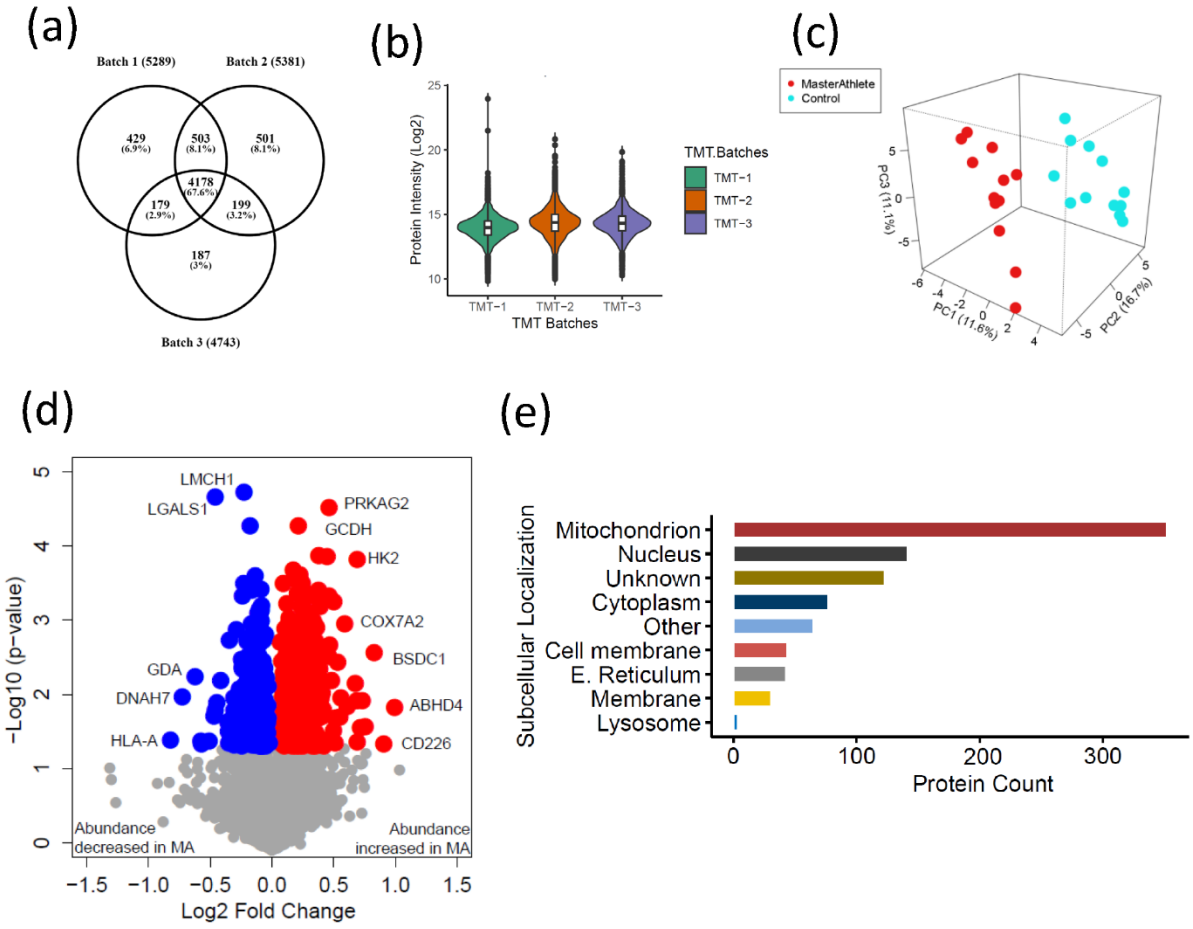

180

181 **2.4 Mitochondrial protein enrichment in octogenarian MA**

182 The 369 mitochondrial proteins overrepresented in MA include 117 mitochondrion inner
183 membrane proteins, 21 outer membrane proteins, 18 matrix proteins, 10 inter-membrane space
184 proteins, and 5 outer membrane proteins. The abundance of all mitochondrion proteins is higher
185 in MA, except 8 proteins (Figure 3a). Enrichment analysis with the whole human genome as a
186 statistical background revealed oxidoreductase activity, electron transport activity, and cofactor
187 binding as the top significantly enriched pathways in MA after FDR correction and fisher exact
188 test cut-off at p<0.01 (Figure 3b). Specifically, 110 proteins associated with TCA and respiratory
189 electron transport, 71 proteins from oxidative phosphorylation and 43 protein constituents of

complex I, 3 in complex II (SDHA, SDHB, SDHC), 8 in complex III, 13 in complex IV, and 10 in complex V were significantly more abundant in MA (Figure 3c).

The cytoplasmic and nuclear SIRTs were not quantified in our dataset; however, we explored SIRT3 and SIRT5 mitochondrial sirtuins, which are master regulators of mitochondrial biology, including energy production, metabolism, apoptosis, and intracellular signaling. Both SIRT3 and SIRT5 proteins were 1.2-fold more abundant in MA than NA ($p<0.01$) (Figure 3d). Of note, the overrepresentations of SIRT3 in MA were consistent with higher deacetylation of long-chain acyl-CoA dehydrogenase (LCAD) in MA (FC 1.14 and $p= 0.007$), which suggest upregulation of lipid catabolism and fatty acid oxidation pathways. The deacetylase activity of SIRT3 improves mitochondrial function by the deacetylation of mitochondrial complex I protein NADH ubiquinone oxidoreductase subunit A9 (NDUFA9) (Ahn *et al.*, 2008) and succinate dehydrogenase from complex II (SDH) (Cimen *et al.*, 2010). SIRT3 also deactylates the mitochondrial permeability transition-regulating protein, cyclophilin D, to reduce likelihood of opening of the mitochondrial permeability transition pore (Hafner *et al.*, 2010). Finally, SIRT3 deacetylates lysine residues on SOD2 to promote its antioxidant activity and thereby reduce the level of ROS released outside mitochondria. Whilst we would expect this deacetylation to increase SOD2 activity independent of changes in SOD2 content, in our study SOD2 protein (FC=1.17, $p= 0.037$) was also more highly expressed in MA. Comparatively, less is known about SIRT5 than SIRT3, but it has been reported that SIRT5 physically interacts with cytochrome c (CYCS) and CYCS abundance was 1.3-fold higher in MA (Figure 3-figure supplement 1, panel a).

Figure 3

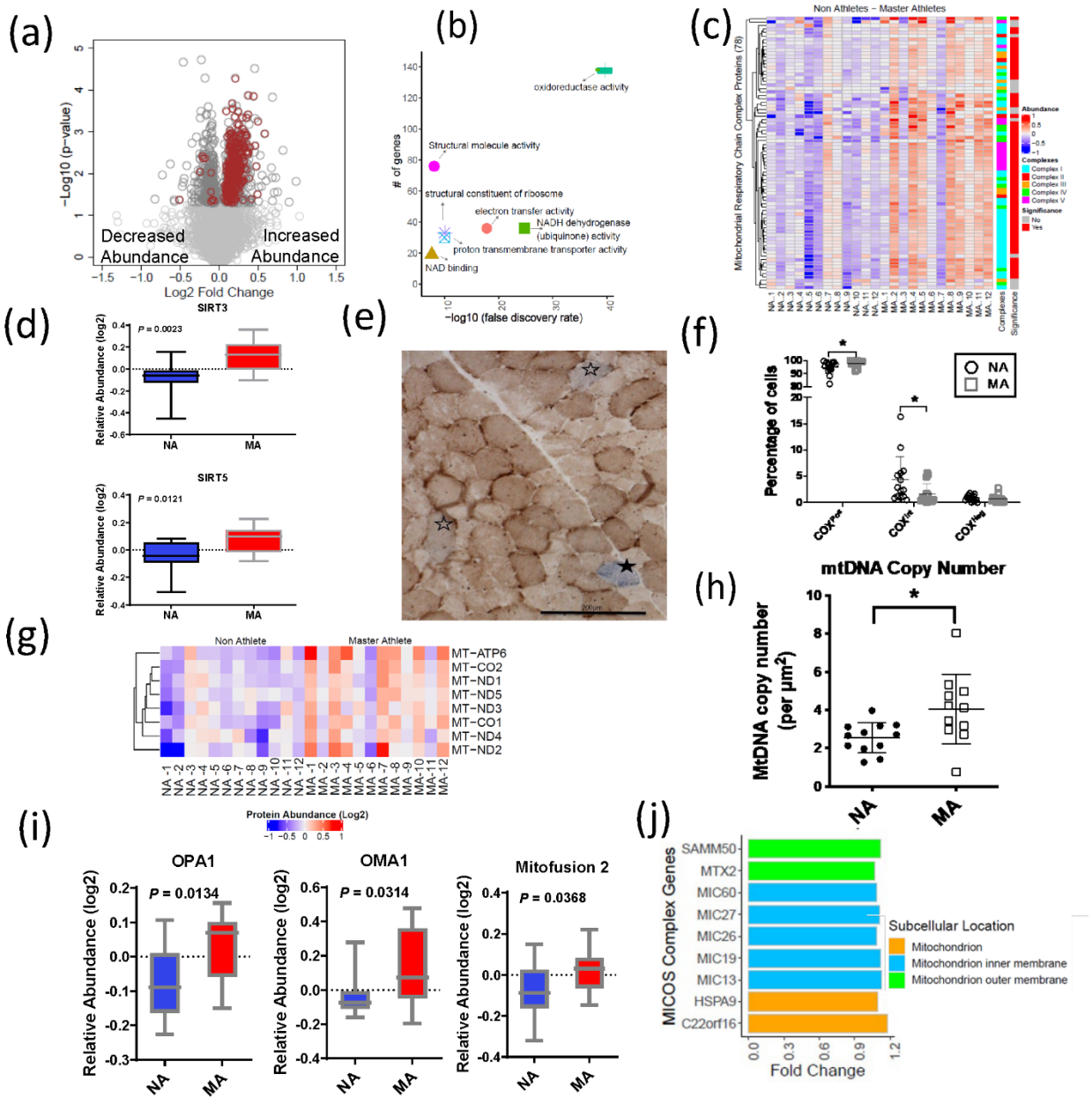

While our proteomics analyses identified a globally higher abundance of OXPHOS proteins (Figure 3c), markers of mitochondrial content specifically assessed by Western blot were not univocally associated with MA status. For example, VDAC was not different between groups, whereas citrate synthase by proteomics was elevated in MA (Figure 3-figure supplement 1, panel b). Furthermore, we observed a significant effect (p=0.046) for a higher abundance of OXPHOS complexes relative to VDAC in MA when analyzed by Western blot, consistent with the higher abundance of OXPHOS complexes by proteomics in MA (Figure 3-figure supplement

1, panel c) (uncut blots for VDAC and Oxphos subunits are shown in (Figure 3-figure supplement 2 -source data 1). Histochemical analysis to quantify muscle fibers with compromised respiratory function revealed a significantly higher abundance of healthy COXPos fibers ($p=0.0291$) and fewer respiratory chain compromised (COXInt) myofibers ($p=0.0448$) in MA (Figure 3e-f). Thus, the proteomics data is consistent with histochemical phenotypic data showing better maintenance of respiratory competent muscle fibers (COXPos fibers) in MA and an increased abundance of ETC subunits ratio relative to VDAC. This latter observation could suggest greater cristae surface area relative to mitochondrial volume, or differences in the clearance of mitochondrial membranes.

In contrast to the general higher abundance of mitochondrial proteins noted above, 8 mitochondrial proteins had a lower abundance in MA, which were: NADH-cytochrome b5 reductase 3 (CYB5R3), Phosphatidate cytidylyltransferase 2 (CDS2), Long-chain-fatty-acid--CoA ligase 3 (ACSL3), Dimethylarginine dimethylaminohydrolase 1 (DDAH1), WD repeat-containing protein 26 (WDR26), Serine/threonine-protein phosphatase PGAM5 (PGAM5), SHC-transforming protein 1 (SHC1), and StAR-related lipid transfer protein 7 (STARD7).

2.5 mtDNA proteins enrichment and maintenance of cristae architecture in octogenarian MA

Previous studies suggest respiratory chain defects in skeletal muscle may result from high levels of mtDNA mutations (Bua *et al.*, 2006b; Murphy *et al.*, 2012a) and/or mtDNA depletion (Muller-Hocker *et al.*, 1993; Mueller *et al.*, 2012). To address this issue in our subjects, we specifically explored mitochondrial proteins in our proteomics dataset encoded in mtDNA. Of the known 13 mtDNA proteins, 8 were quantified in our data, and all of them were significantly more abundant in MA than in NA ($p<0.05$) (Figure 3g). The proteomics data were consistent with findings that absolute mtDNA copy number evaluated using a quantitative method was higher in MA than in NA (Figure 3h) and indicated parallel protection of mtDNA copies and mtDNA-encoded proteins in MA. Further, the observation of a lower abundance of respiratory compromised fibers (defined as low or absent complex IV staining in COX-SDH double-stained muscle cross-sections) (Figure. 3e,f) in MA versus NA is consistent with a lower burden of mtDNA mutation in highly functioning MA octogenarians compared to NA.

Consistent with the higher protein levels of many mitochondrial proteins in MA, our results show that 38 proteins from 28S and 39S mitoribosomal proteins were significantly more abundant in MA, suggesting an increased mitochondrial protein synthesis. Conversely, cytoplasmic

ribosomal protein (RPS2, RPLP0) abundance was lower in MA (Figure 3-figure supplement 1, panel d).

Mitochondrial morphology is regulated by proteins that modulate fission (e.g., DRP1) and fusion (e.g., OPA1, MFN 1 & 2). For example, OPA1 induces mitochondrial inner membrane fusion (Mishra *et al.*, 2014) to promote cristae tightness, increase the activity of respiratory enzymes and enhance the efficiency of mitochondrial respiration (Cogliati *et al.*, 2013). Interestingly, OPA1, MFN1, and DRP1 were overrepresented in MA (Figure 3i), although DRP1 fold elevation in MA donors was not statistically significant. The mitochondrial contact site and cristae organizing system (MICOS) complex are crucial for maintaining cristae architecture, and knockdown of MICOS components leads to mitochondria with altered cristae morphology and compromised oxidative phosphorylation. In this study, 15 out of 17 Uniprot annotated MICOS complex proteins were quantified, and 9 of them were significantly more abundant in MA (Figure 3j). For example, the mitochondrial inner membrane protein mitofilin (MIC60), which controls cristae morphology and is thus indispensable for normal mitochondrial function (John *et al.*, 2005), was 1.2 times fold more abundant in MA donors. Of note, we have previously reported a decrease in the abundance of these 9 proteins with healthy aging (Ubaida-Mohien *et al.*, 2019b).

A complex array of dynamic protein interactions (Sam50, Metaxin, and the inner membrane localized MICOS) at cristae junctions that form the Mitochondrial Intermembrane Space Bridging (MIB) complex was reported recently (Huynen *et al.*, 2016). The outer mitochondrial membrane protein Metaxin2 (MTX2), which was significantly more abundant in MA (Figure 3-figure supplement 3, panel a), interacts with MICOS complex and MTX3, which are the part of MIB complex (Huynen *et al.*, 2016). Metaxins, together with Sam50, are also important for the stability of respiratory complexes (Ott *et al.*, 2012). A general translocase mediates the import of nuclear-encoded mitochondrial preproteins in the outer membrane, the TOM complex, and by two distinct translocases in the mitochondrial inner membrane, the TIM23 complex, and the TIM22 complex. The average expression of two TOM complex proteins (TOMM22 and TOMM40) and ten TIM complex proteins (TIM10, TIM13, TIM14, TIM16, TIM22, TIM23, TIM29, TIM44, and TIM50) were found to be more abundant in MA (Figure 3-figure supplement 3, panel b).

2.6 Autophagy and proteostasis pathway proteins in octogenarian MA

Skeletal muscle mass is influenced by the proteolytic process of protein turnover and degradation. The major regulatory process of the proteolytic system is chaperone mediated autophagy by lysosomes, and the ubiquitin proteasome pathway. There were 267 proteins from these pathways quantified, and 47 proteins were significantly associated with MA ($p<0.05$, 17 underrepresented in MA). The proteins were categorized as Autophagy, Autophagy-Lysosome, Chaperones, Proteasome, and other proteostasis cluster proteins (Figure 3-figure supplement 4). Proteasome proteins PSMB1, PSMA2, small heat shock protein HSPB8, DNAJ proteins like DNAJB4, DNAJC3 etc., were lower in MA. Activation/inhibition of autophagy – such as V-type proton ATPase 116 kDa subunit isoform 1 (ATP6V0A1), Heat shock 70 proteins like HSPA2 and HSPA1A proteins, were also lower in MA. A lower ATP6V0A1 was reported previously in highly active aging healthy donors (Ubaida-Mohien *et al.*, 2019a). In contrast, many mitochondrion localized proteostasis proteins like HSCB, MRPL18, TIMM9, HSPE1, HSPA9 etc., were higher in abundance in MA. PRKAG2, 5′-AMP-activated protein kinase subunit gamma-2, a component of AMP kinase main energy-sensor protein kinase that responds to changes in the cellular AMP:ATP ratio and regulates the balance between ATP production and consumption, was one of the highly expressed proteins (log2FC 1.3) in MA octogenarians, suggesting a tightly monitored balance between energy production and utilization (Mounier *et al.*, 2015).

2.7 Impact of nuclear pore membrane proteins and transport proteins in octogenarian MA

Nuclear pore complexes (NPCs) facilitate and regulate the transport of different macromolecules across the nuclear envelope, allowing bilateral exchanges between the nuclear and the cytoplasmic environment (Strambio-De-Castillia *et al.*, 2010; Wente & Rout, 2010). 25 nuclear pore proteins were quantified, all less expressed in MA than in NA, and for 12 of them, the difference was statistically significant ($p<0.05$) (Figure 3-figure supplement 5, panel a). Nucleopore cytoplasmic filaments like NUP358, NUP98 and NUP88, and adaptor NUPs like NUP98/96 were less abundant in MA. Tpr, the central architectural element of nuclear pore formation, Nup93, which is critical for nuclear permeability, were also less abundant in MA (Figure 3-figure supplement 5, panel b). The lower abundance of proteins of the nuclear pore in MA was unexpected and should be further explored in future studies.

2.8 Spliceosome pathway proteins are under-represented in octogenarian MA

Alternative splicing produces protein variants by combining information from different exon sequences in the same genes. Aging is associated with the emergence of different splicing variants of the same genes (Harries *et al.*, 2011; Holly *et al.*, 2013; Bhadra *et al.*, 2020). However, it remains unknown whether these changes in the human proteome are part of the aging process or represent resilience strategies to cope with the damage accumulation and functional decline associated with aging (Deschenes & Chabot, 2017). Previous studies have shown that alternative splicing is particularly abundant in skeletal muscle, and we have shown that proteins that regulate alternative splicing are significantly overrepresented in skeletal muscle tissue from older compared to younger healthy individuals (Ubaida-Mohien *et al.*, 2019b). Interestingly, after accounting for age and other covariates, being physically active in daily life was associated with a lower representation of spliceosome proteins in skeletal muscle (Ubaida-Mohien *et al.*, 2019a). Also, one of the strongest signals in this analysis was a lower representation of proteins related to mRNA metabolic process, mRNA splicing, and mRNA processing in MA. In particular, we were able to quantify 132 spliceosome proteins, 102 proteins were less abundant in MA, and 22 proteins were significantly less abundant in MA ($p<0.05$) (Figure 4a). The functional characteristics of the spliceosomal proteins were shown in (Figure 4b). Of note, TRA2A, an RNA-binding splicing factor protein that modulates splicing events and translation, was among the most significantly affected proteins ($p=0.0004$) in this category with the greatest fold-difference from NA (Figure 4c). Functional analysis of TRA2A suggests a highly interconnected functional interaction network with two major pathway proteins: mRNA splicing major pathway (red), and mRNA splicing minor pathway (blue) proteins (Figure 4d). Despite not having a direct interaction within this network, the DCPS protein has a role in the first intron splicing of pre-mRNAs (Figure 4d). Taken together, the lower representation of spliceosome proteins that regulate alternative mRNA splicing in MA are consistent with the effects of physical activity in our previous study and suggest that alternative splicing is part of a resilience response in the face of lower mitochondria function. Such a resilience response is not required in MA because of high mitochondrial function maintenance despite old age (Ubaida-Mohien *et al.*, 2019a). This hypothesis is consistent with previous data showing that after adjusting for age and physical activity, better skeletal muscle oxidative capacity assessed by ^{31}P-MR spectroscopy is associated with overrepresentation of splicing machinery and pre-RNA processing proteins (Adelnia *et al.*, 2020).

Figure 4

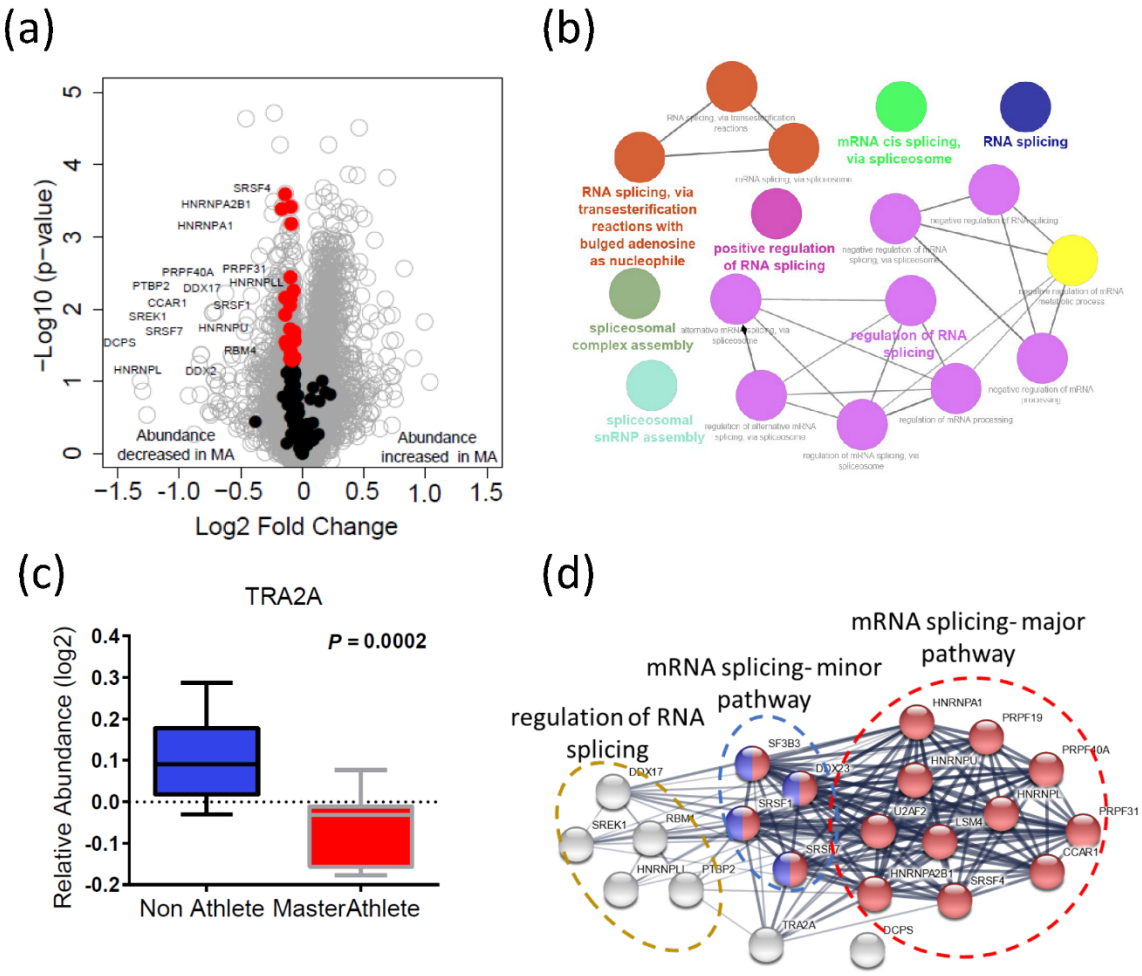

2.9 Modulation of mitochondrion and splicing machinery with aging, physical activity, and exercise

To further explore the hypothesis that alternative splicing is part of a compensatory adaptation to impaired mitochondrial function, we combined the results of this study with the skeletal muscle proteomic data in 58 healthy participants collected in the GESTALT study (Figure 5–figure supplement 1) (Ubaida-Mohien *et al.*, 2019a; Ubaida-Mohien *et al.*, 2019b). Notably, we searched for proteins that were underrepresented with age (GESTALT, Age-) and overrepresented with both higher physical activity (GESTALT, PA+) and in Master Athletes (MA+) compared to age-matched controls (Figure 5). Enrichment analysis of proteins at the intersection showed 50 proteins enriched at all three shared interceptions, including proteins representing mitochondrial biogenesis, TCA cycle and respiratory electron transport, MICOS complex, and cristae formation (Figure 5).

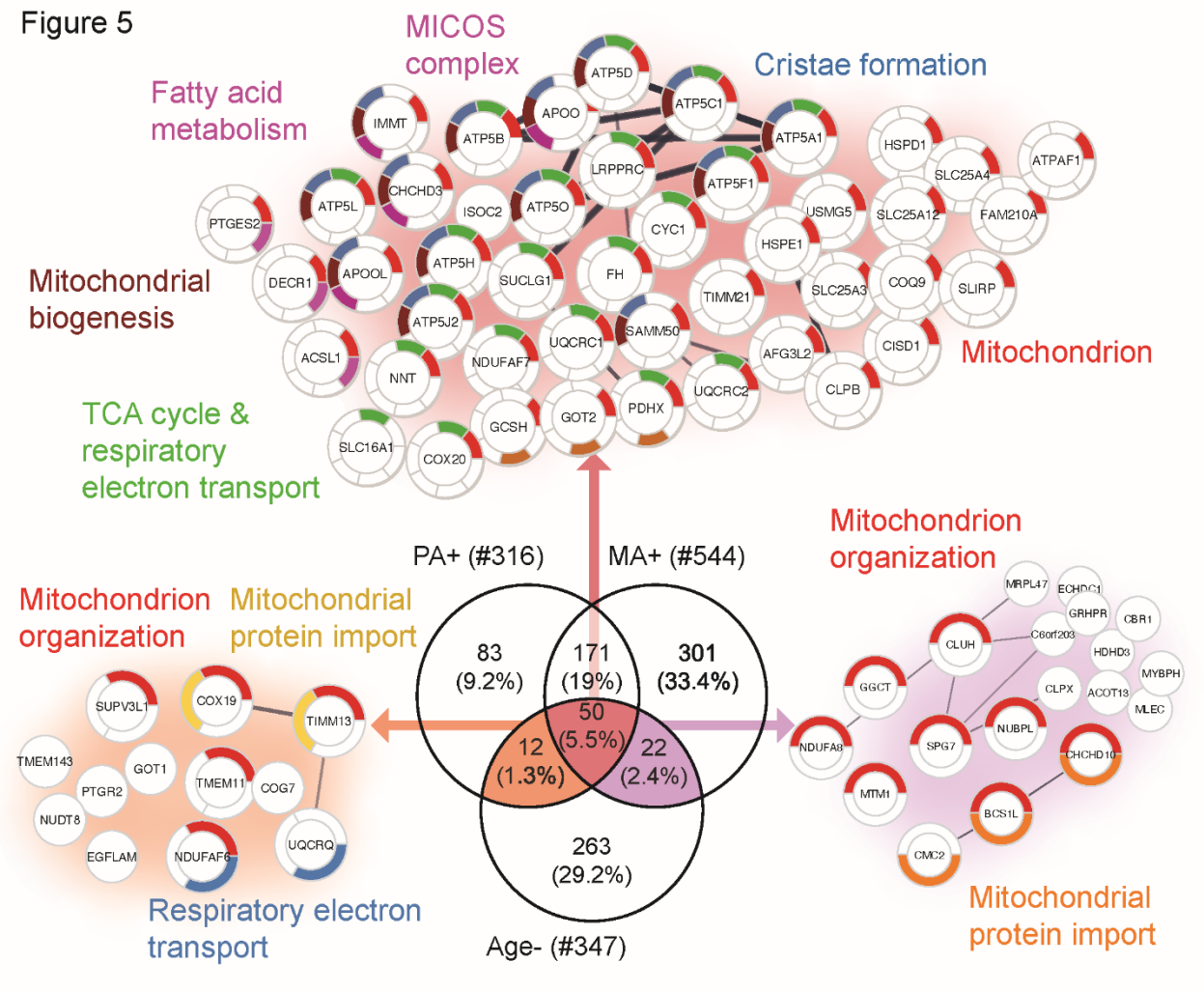

Although there was considerable overlap between proteins overrepresented with higher physical activity in the GESTALT study and proteins overrepresented in MA, a large group of proteins related to mitochondrial protein import and mitochondrion organization were specific to the MA group (not associated with physical activity *per se*). This suggests that although many of the proteins which are more abundant in MA versus NA can be attributed to MAs physical activity habits, this does not account for all of the differences observed. Specifically, out of 301 unique MA+ proteins, a subset of proteins: mitochondrial translation (36 proteins), mitochondrial inner membrane (75 proteins), mitochondrial matrix proteins (65 proteins) appear unrelated to physical activity and may reflect unique biology in our MA group (Figure 6).

367 **Figure 6**

368

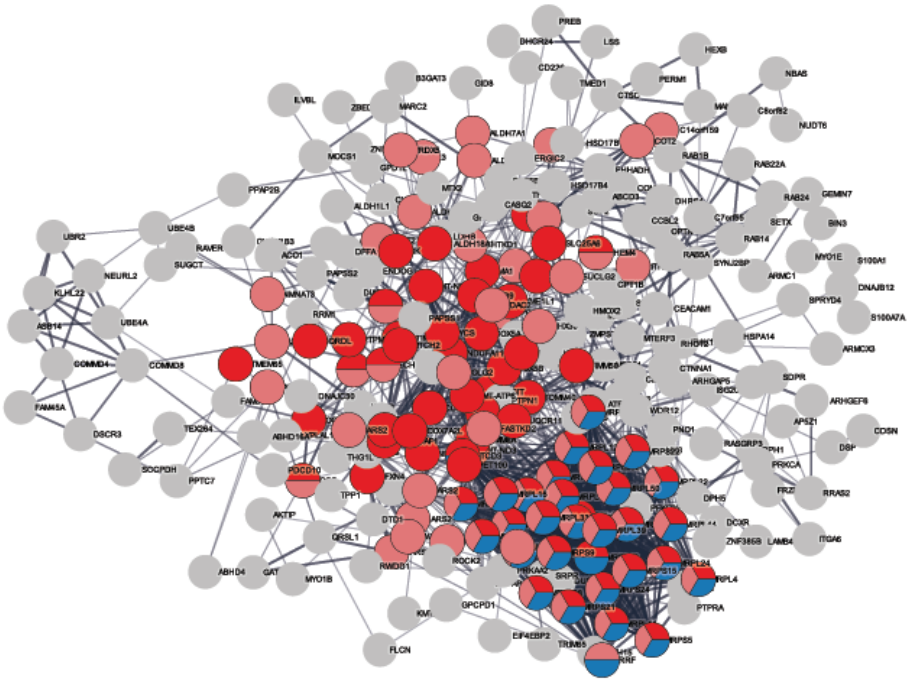

379 In the next analysis, we considered the proteins which were overrepresented with age
380 (GESTALT, Age+) and underrepresented with both higher physical activity (GESTALT, PA-) and
381 in Master Athletes (MA-) compared to age-matched controls (Figure 7 panel a). Interestingly, we
382 found 40 proteins in all three meaningful interceptions (Age+/PA-/MA-; Age+/PA-/; Age+MA-),
383 and these involved mRNA splicing, capped introns containing pre-RNA, sarcolemma, regulation
384 of glucokinase, spliceosome, and metabolism of RNA (Figure 7). The other notable category
385 pathway differentially represented in Age+ and MA- were the NLRP inflammasome pathway,
386 indicating the inflammasome proteins that increase with aging are antagonized in MA subjects.
387 Although more proteins were affected in PA than MA versus NA, several proteins were affected
388 in MA versus NA that were not affected by PA, supporting the idea that there are likely factors
389 beyond physical activity involved in protecting the MA group's muscle proteome. Specifically,
390 162 MA-exclusive proteins were under-represented in MA vs NA and reflect the unique
391 physiology of MA participants. Enrichment analysis identified proteins regulating nuclear pore
392 organization (NUP133, NUP153, NUP54), heterochromatin organization (HP1BP3, H3F3B and
393 HMGA1) and telomere (HMBOX1, PURA, TERF2IP), mRNA and splicing process, and
394 contractile/sarcomere fiber proteins (Figure 7 panel b, Table S3).

Figure 7

(a)

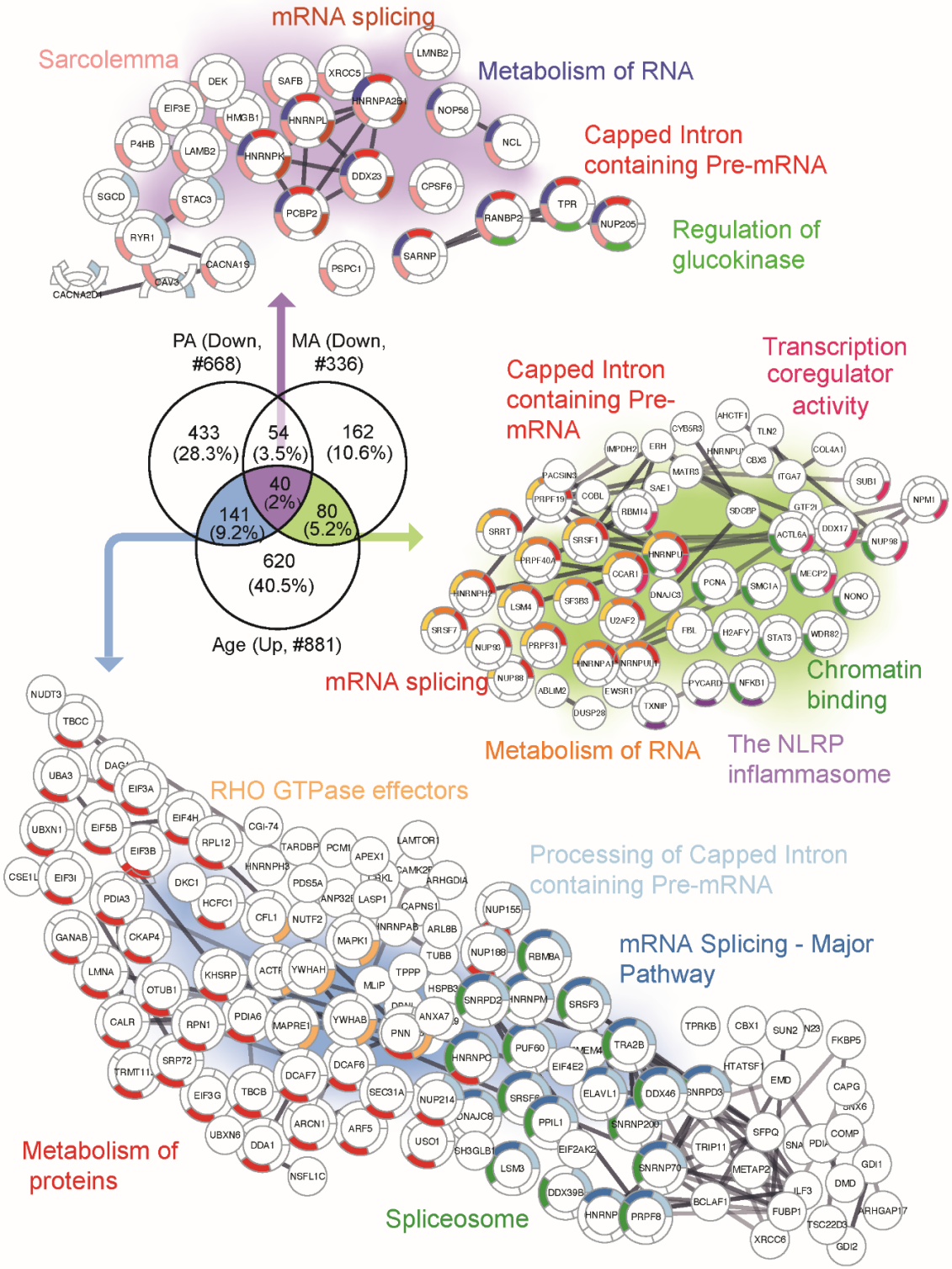

(b)

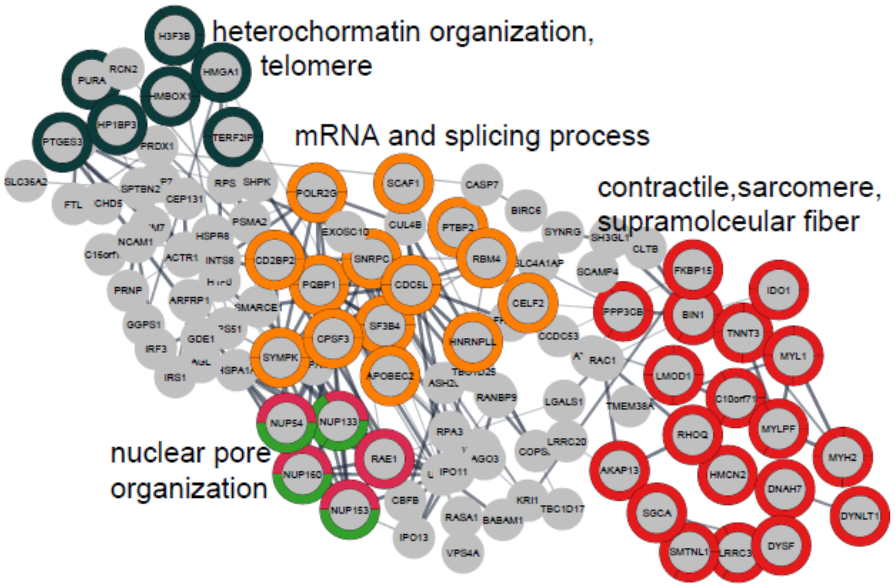

3 DISCUSSION

Mass spectrometry-based proteomics studies strongly suggest in a select group of individuals free of major disease risk factors and morbidity, that skeletal muscle mitochondrial proteins are underrepresented in older compared to younger persons, and, independent of age, are over-represented in those who are more physically active in daily life (Kleinert *et al.*, 2018; Ubaida-Mohien *et al.*, 2019a; Ubaida-Mohien *et al.*, 2019b). In this respect, these prior studies suggest that aging and physical activity have opposite effects on mitochondrial health. However, as most individuals' level of physical activity declines with aging, a clear-cut dissection of the effect of aging independent of declining physical activity has proven difficult to achieve. To address this question, 15 exceptionally fit and physically very active octogenarian MA were compared to 14 healthy but non-athletic octogenarian NA. In accordance with our hypothesis, we found a massive overrepresentation of mitochondrial proteins and these data were consistent with the finding of higher mtDNA copy number, fewer respiratory chain compromised muscle fibers by histochemistry, and an increased ratio of mitochondrial inner membrane-bound ETC subunits relative to the outer mitochondrial membrane protein VDAC in skeletal muscle of MA octogenarians. We also found a lower abundance of proteins regulating RNA splicing in MA, confirming that in older persons with high mitochondrial function, the upregulation of the splicing machinery usually observed with older age is not occurring (Ubaida-Mohien *et al.*, 2019b).

In general, we found that many proteins overrepresented in MA were similar to the proteins that have been associated with higher physical activity in daily life, independent of age in previous studies (Ubaida-Mohien *et al.*, 2019a). These findings demonstrate that some of the biological mechanisms that facilitate the high function of our octogenarian MAs in spite of old age are similar to those beneficially affected by moderate physical activity in skeletal muscle (Nilsson & Tarnopolsky, 2019). However, we also found differentially represented proteins in highly functioning octogenarian MA that were unique from those affected by physical activity, suggesting unique biological mechanisms also contribute to the extreme performance capacity in this select group of individuals. This unique set of proteins unrelated to physical activity may provide novel insight on mechanisms, either genetic and/or linked to life-course exposure, that may counteract the physical function decline that is observed in the great majority of aging individuals. In total, we found 176 proteins related to mitochondria that were over-represented in MA versus NA that had not been previously linked to physical activity. For example, amongst these, 22 proteins which mediate mitochondrial protein import and are involved in establishing and modulating the mitochondrial architecture were over-represented in MA but had not been previously reported as affected by physical activity (Ubaida-Mohien *et al.*, 2019a).

A striking result of this study, is that 80 proteins involved with mRNA splicing, metabolism of RNA, capped intron containing pre-RNA and transcription coregulator activity that were shown previously to significantly increase with aging (Rodriguez *et al.*, 2016; Ubaida-Mohien *et al.*, 2019b) were globally underrepresented in MA. These data are consistent with previous suggestions that the production of alternative splicing variants of structural and regulatory proteins are an integral part of the pre-programmed resilience strategies aimed to counteract drifts toward loss of function and damage accumulation, such as those that follow the decline of energy availability secondary to mitochondrial impairment (Bhadra *et al.*, 2020).

Mitochondria and Aging Skeletal Muscle

Mitochondria have long been implicated in aging biology in general, including skeletal muscle aging. Mitochondrial derangement may contribute to functional decline with aging though various mechanisms, including but not limited to reduced energy availability for contraction and other essential cellular activities, increased production of reactive oxygen species, inflammatory signaling, and release of Ca^{2+} and activation of caspase 3 consequent to an event known as mitochondrial permeability transition (Hepple, 2016). In addition, fragments of mitochondrial membrane or mtDNA may trigger the NLRP3 inflammasome and contribute to local and

systemic inflammaging (Pereira *et al.*, 2019). Hence, preserving skeletal muscle mitochondrial function is a central mechanism for maintaining skeletal muscle health with aging.

Further, mitochondrial proteins that cover a large variety of locations and functions were more abundant in highly functioning octogenarians than controls, including signaling proteins that fine-tune mitochondrial dynamics, mitochondrial biogenesis, TCA cycle, and respiratory electron transport. Evidence in the literature suggests that most of these changes are a consequence of higher physical activity (Ubaida-Mohien *et al.*, 2019a). In keeping with this view, we recently showed that a reduction in intrinsic mitochondrial respiratory capacity (respiration normalized to the abundance of a complex III subunit) was only seen in very sedentary but not in physically active septuagenarian men (Spendiff *et al.*, 2016), and data from the literature show that low physical activity rather than aging *per se* causes an increase in skeletal muscle mitochondrial ROS emission (Gram *et al.*, 2015).

The mechanisms by which physical activity attenuates oxidative stress are complex and not completely understood. On the one hand, the promotion of autophagy and mitochondrial biogenesis jointly contribute to the recycling of damaged mitochondria and subsequent replacement with healthy mitochondria that are less likely to generate excessive ROS. On the other hand, exercise in MA likely upregulates enzymatic antioxidants such as SOD2 by a NRF2-KEAP1 mechanism (Gao *et al.*, 2020). Although our proteomic analysis did not detect PGC-1α, we did observe an increase in MA skeletal muscle for *PGC-1 and ERR-induced regulator in muscle protein 1* (PERM1), a regulator of mitochondrial biogenesis (Cho *et al.*, 2016). In addition, the mitochondrial SIRT3 was elevated in MA muscle. Exercise activates SIRT3 by an AMP-activated protein kinase-dependent mechanism (Brandauer *et al.*, 2015), and, in turn, SIRT3 deacetylates the mitochondrial antioxidant enzyme SOD2 boosting its ROS-scavenging activity (Tao *et al.*, 2010). This is consistent with a previous study where they also reported a significantly higher level of SIRT3 and SOD2 in the skeletal muscle of master athletes (~15 y younger than studied here) compared to age-matched controls (Koltai *et al.*, 2018). Finally, mitochondrial permeability transition is an important source of elevated mitochondrial ROS in skeletal muscle (Burke *et al.*, 2021) and SIRT3, which was elevated in MA, reduces mitochondrial permeability transition by deacetylation of cyclophilin D (Hafner *et al.*, 2010).

The differential representation of proteins that fine-tune mitochondrial dynamics between MA and NA is particularly interesting because an optimal dynamic balance of expression between pro-fusion (OPA1, MFNs) (Tezze *et al.*, 2017) and pro-fission (DRP1) processes (Dulac *et al.*,

2020) is essential for mitochondrial health. Consistent with this idea, our data showed a higher abundance of pro-fusion (OPA1, MFN2) and pro-fission (OMA1) proteins, as well as a higher abundance of mitochondrial electron transport complex assembly proteins (NUBPL, COA1, ACAD9, etc.) in MA donors. Collectively, the higher abundance of these proteins in MA suggests better maintenance of processes involving mitochondrial dynamics and cristae remodeling in MA. In addition, maintained mitochondrial dynamics is also likely conducive to the better preservation of mtDNA that we observed in MA, given the importance of mitochondrial dynamics to mtDNA integrity (Bess *et al.*, 2012). Importantly, our proteomics data are consistent with phenotypic data showing a higher abundance of respiratory competent muscle fibers and higher mtDNA copy number in MA versus NA. Interestingly, there were 8 mitochondrial proteins that had a lower abundance in MA than can be expected by random chance. However, 4 of these proteins were associated with GO Biological Process lipid biosynthesis (CYB5R3, CDS2, ACSL3, and STARD7). CDS2 is an essential intermediate in the synthesis of phosphatidylglycerol, cardiolipin, and phosphatidylinositol (PI), an important regulator of lipid storage (Qi *et al.*, 2016). STARD7 is an intramitochondrial lipid transfer protein for phosphatidylcholine. These data are generally consistent with a recent magnetic resonance spectroscopy analysis of aging human muscle, showing that elderly subjects who did not exhibit significant muscle atrophy had lower levels of skeletal muscle phospholipids (Hinkley *et al.*, 2020). The other 4 proteins that had lower expression in MA were PGAM5 (regulator of mitochondrial dynamics), Dimethylarginine dimethylaminohydrolase 1 (DDAH1), SHC1(mitochondrial adapter protein), and WDR26 (negative regulator in MAPK signaling pathway). The significance of the lower expression of these proteins in MA is unclear. Of note, most of these proteins are primarily located in the endoplasmic reticulum, although they are also found in mitochondria. WDR26 is expressed mostly during mitochondrial stress and hypoxia, which is less likely to occur in MA compared to controls. The underrepresentation in MA of STARD7, a protein important to efficient phosphatidylcholine import by mitochondria as well as mitochondrial function and morphogenesis, may be considered counterintuitive. However, recent studies have suggested that STARD7 is a candidate effector protein of ceramide, a lipid known for its ability to initiate a variety of mitochondria-mediated cytotoxic effects. Thus, the downregulation of STARD7 in MA may be a compensatory strategy (Bockelmann et al., 2018).

In summary, our data suggest that overrepresentation of mitochondrial quality control proteins and mitochondrial dynamics proteins in octogenarian MA muscle likely translates to better

maintenance and remodeling of mitochondrial cristae, with higher energy availability that positively affects cellular adaptation to stress, and better maintenance of muscle metabolism.

RNA Splicing, Nuclear Pore Complex, and Aging.

Amongst the notable findings of our study is that 80 proteins involved with mRNA splicing, metabolism of RNA, capped intron containing pre-RNA and transcription coregulator activity that were shown previously to significantly increase with aging (Rodriguez *et al.*, 2016; Ubaida-Mohien *et al.*, 2019b) were globally underrepresented in MA compared to controls. Interestingly, after accounting for physical activity and age, we previously found that upregulation of spliceosome proteins is associated with higher mitochondrial oxidative capacity as measured by 31P-spectroscopy (Adelnia *et al.*, 2020). Thus, the lower representation of spliceosome proteins that regulate alternative mRNA splicing in MA, coupled with the positive association between the spliceosome and mitochondrial oxidative capacity independent of age and physical activity status that we observed previously (Adelnia *et al.*, 2020), collectively suggest that alternative splicing may be part of a resilience response in the face of lower mitochondrial function with aging. Such a resilience response is not required in MA because of high mitochondrial function maintenance despite old age. Future analysis of RNA expression to examine expression of splice variants in MA versus NA would be important to further evaluate this premise.

An unexpected finding was that nuclear pore complex proteins were less represented in MA than controls. The nuclear pore complex proteins are involved in mRNA splicing regulation (Stewart, 2019), and therefore under-representation of nuclear pore complex proteins in MA may be part of a global down-regulation of splicing. In this respect, since post-translational oxidative modification and activation of mitochondrial-mediated apoptotic pathways are associated with upregulation of nuclear pore complex proteins (Lindenboim *et al.*, 2020), a higher level of mitochondrial function in MA probably requires less protein turnover and thus less synthesis of nucleoporins and structural proteins. This idea is consistent with the discordant responses of mitochondrial versus non-mitochondrial ribosomal proteins, where we observed that 38 mitochondrial ribosomal proteins from 28S and 39S were significantly higher expressed in MA, whereas cytoplasmic ribosomal proteins (RPS2, RPLP0) were less abundant in MA.

Proteostasis maintenance pathways are important for skeletal muscle, as components of myofibers are often damaged and must be replaced regularly. Proteins involved in proteostasis appear to have no single trend of change in MA octogenarians, with some chaperones and

552 autophagy proteins underrepresented and some overrepresented in MA. It is possible that the
553 long-term physical activity adaptation of the skeletal muscle in MA reduces the need for
554 replacement of muscle proteins, e.g., the higher fidelity of their mitochondria coupled with the
555 higher expression of antioxidant proteins such as SOD2 may limit post-translational damage to
556 proteins, thereby reducing the rate at which they need to be replaced.

557 *Evidence for Factors Other than Exercise in MA Proteome*

558 To a large extent the results of this study are consistent with the well-established benefits of
559 exercise on mitochondrial and skeletal muscle health (Hood *et al.*, 2019). However, the
560 individuals we studied were world-class athletes in their eighties and it is unlikely that their high
561 function can be accomplished by the majority of older people, even assuming that they adhere
562 to a strict exercise regimen. We expect that a fortuitous combination of genetics and
563 environmental factors beyond exercise *per se* make them *winners*. Consistent with the idea that
564 factors beyond those linked to physical activity contribute to such an extreme phenotype, we
565 observed several mitochondrial-related proteins that were uniquely upregulated in MA versus
566 normal aging, and several proteins involving RNA processing and the inflammasome that were
567 uniquely down-regulated in MA versus normal aging. As these proteins are not amongst those
568 previously identified as exercise-responsive (Ubaida-Mohien *et al.*, 2019a), we refer to these as
569 the MA-specific proteome (see Figure 6 and 7). Although our MA cohort is too small to permit
570 assessment of genetic/hereditary factors in these protein differences, our results identify
571 important candidate protein pathways to explore for anti-aging effects and suggest additional
572 studies with larger numbers of subjects (and including other types of athletes) would be
573 worthwhile.

574 *In conclusion*, our data underscore that mitochondrial pathways are key to maintaining a high
575 level of physical function in advanced age. Furthermore, our data show that high physical
576 function is also associated with preventing the general increase with aging in nuclear pore
577 complex proteins and spliceosome proteins. Whereas many of the differentially represented
578 proteins in MA overlap with those affected by daily physical activity, we also identified several
579 proteins that typically change with aging and were uniquely countered by MA but not by physical
580 activity. The study of these unique proteins may reveal mechanisms that allow sporadic
581 individuals to maintain high level of physical activity late in life, and understanding these
582 mechanisms may indicate new therapeutic strategies for attenuating sarcopenia and functional
583 decline with aging.

4 MATERIALS & METHODS

4.1 Ethical approval

All procedures carried out with human subjects were done with prior approval from the Institutional Review Board of the Faculty of Medicine at McGill University (A08-M66-12B) and according to the Declaration of Helsinki. All subjects provided written informed consent.

4.2 Human subject characteristics

Age- and sex-matched octogenarian world-class track and field athletes (n=15; 8 female) and non-athlete participants (n=14, 6 female) were recruited for this study. No explicit power analysis was performed *a priori* due to the rare nature of the octogenarian world class athletes, but the premise was to select populations of widely different physical function in advanced age so that insights concerning the role of potential differences in muscle biology in the differences in physical function might be obtained.

4.3 Sample collection

Muscle cross-sectional area by MRI and a vastus lateralis muscle biopsy were performed in 15 octogenarian world-class track and field athletes and 14 non-athlete age- and sex-matched non-athlete controls. A portion of muscle from a subset of 12 master athletes (MA mean age 81.19 ± 5.1 y) and 12 non-athlete controls (NA mean age 80.94 ± 4.5 y) was used from these subjects for liquid-chromatography mass spectrometry to generate quantitative tandem mass tag proteomics data. In addition, we measured muscle mass by MRI, mtDNA copy number, and western blot of oxidative phosphorylation proteins.

4.4 Muscle fiber type labeling and imaging in muscle cross-sections

Ten-µm thick sections that were serial to those used in histochemical labeling for respiratory compromised fibers were used in immunolabeling experiments to demonstrate fiber type by probing for the major myosin heavy chain (MHC) isoforms in human skeletal muscle. Sections were first hydrated with 1 x phosphate buffered saline (PBS) and blocked with 10% normal goat serum for 30 min in 1 x PBS. Sections were subsequently incubated with the following primary antibodies for 1 h at room temperature: polyclonal rabbit anti-laminin IgG (L9393, 1:700; Sigma-Aldrich), monoclonal mouse anti-MHCI IgG2b (BA-F8, 1:25), monoclonal mouse anti-MHCIIa IgG1 (Sc71, 1:200), and monoclonal mouse anti-MHCIIx IgM (6H1, 1:25). MHC primary antibodies were obtained from the Developmental Studies Hybridoma Bank (University of Iowa,

USA). Tissue sections then underwent 3 washes in 1 x PBS, and subsequent incubation with the following secondary antibodies for 1 h at room temperature: Alex Fluor 488 goat anti-rabbit IgG (A11008, 1:500), Alexa Fluor 350 goat anti-mouse IgG2b (A21140, 1:500), Alex Fluor 594 goat anti-mouse IgG (A21125), and Alexa Fluor 488 goat anti-mouse IgM (A21042, 1:500).

Following immunolabeling experiments, slides were imaged with a Zeiss Axio Imager M2 fluorescence microscope (Carl Zeiss, Germany) and analyzed by ImageJ (National Institutes of Health, USA) by an observer blinded to the identity of the samples. An average of 366 $\pm$ 131 fibers were analyzed per sample.

4.5 Histochemical labeling for respiratory compromised muscle fibers

COX/SDH histochemistry (Old & Johnson, 1989; Taylor *et al.*, 2003) was performed to assess the activity of OXPHOS complexes IV (COX) and II (SDH), and thus identify muscle fibers with a respiratory chain deficiency (COX^{Neg}). The COX incubation medium was prepared by adding 100 µM cytochrome *c* to 4 mM of 3,3-diaminobenzidine tetrahydrochloride (DAB) with 20 µg of catalase. Further method details are included here (Supplemental Methods). Counts of COX positive (COX^{Pos}), COX^{Int}, and COX^{Neg} myofibers were performed for the whole muscle cross-section. COX negative fibers are indicative of cells with high levels of mtDNA mutations and will thus not demonstrate the brown reaction product (oxidized DAB) during the first incubation but will stain blue following the second incubation for SDH activity. This is because the nuclear DNA entirely encodes SDH, so any mtDNA mutations will not affect its activity. In contrast, mtDNA mutations could affect complex IV activity and prevent DAB oxidation if a mutation affects a region of mtDNA containing the Cox subunit genes.

4.6 Mitochondrial DNA copy number

Groups of 25 fibers (5 x 5 fibers) in an unstained 20-µm thick muscle cross-section from each subject were randomly selected (random number generator & numbered grid), laser captured, and their DNA extracted using the lysis method and stored at -20°C. The products were then separated and the bands visualized using a G-Box chem imaging system (Figure 3-figure supplement 6-source data1, panel A). The mtDNA fragment was extracted and the total mtDNA copy number in muscle fibres was determined using a standard curve (Greaves *et al.*, 2010) (Figure 3-figure supplement 6-source data 1, panel B). The method details are in Supplemental Methods.

4.7 Sample preparation and protein extraction for MS

Roughly, 5 to 8 mg of vastus lateralis muscle tissue per subject was pulverized in liquid nitrogen and mixed with the modified SDT lysis buffer (100 mM Tris, 140 mM NaCl, 4% SDS, 1% Triton X-114, pH 7.6 (Sigma)) (Wisniewski *et al.*, 2009). Tissues were sonicated, protein concentration was determined, and the sample quality was confirmed using NuPAGE®. 300 µg of muscle tissue lysate was used for tryptic digestion. Samples were basic reverse phase fractionated and analyzed in nano LCMS/MS (Q-Exactive HF) using previously published method (Ubaida-Mohien *et al.*, 2019b). The method details are in Supplemental Methods.

4.8 Proteomics informatics

The raw MS data acquired from 24 samples (MA=12, NA=12) is converted to mgf files (using MSConvert, ProteoWizard 3.0.6002) for each sample fraction and was searched with Mascot 2.4.1 and X!Tandem CYCLONE (2010.12.01.1) using the SwissProt Human sequences from Uniprot (Version Year 2017, 20,200 sequences, appended with 115 contaminants) database. The search engine was set with the following search parameters: TMT 10-plex lysine and n-terminus as fixed modifications and variable modifications of carbamidomethyl cysteine, deamidation of asparagine and glutamate, carbamylation of lysine and n-terminus, and oxidized methionine. A peptide mass tolerance of 20 ppm and 0.08 Da, respectively, and two missed cleavages were allowed for precursor and fragment ions in agreement with the instrument's known mass accuracy. Mascot and X!Tandem search engine results were analyzed in Scaffold Q+ 4.4.6 (Proteome Software, Inc,). The TMT channels' isotopic purity was corrected according to the TMT kit. Peptide and protein probability was calculated by PeptideProphet and ProteinProphet probability model (further details in Supplemental Methods).

The log2 transformed reporter ion abundance was normalized by median subtraction from all reporter ion intensity spectra belonging to a protein across all channels. Relative protein abundance was estimated by the median of all peptides for a protein combined. Protein sample loading effects from sample preparations were corrected by median polishing, i.e., subtracting the channel median from the relative abundance estimate across all channels to have a median zero as described elsewhere (Herbrich *et al.*, 2013) (Kammers *et al.*, 2015). Quantified proteins were annotated, and corresponding gene names were assigned to each protein for simplicity and data representation. Annotation of the proteins was performed by manual curation and combining information from Uniprot, GO, and Reactome database. Further bioinformatics analysis was performed using R programming language (3.4.3) and the free libraries available

on Bioconductor. The validation of the age effects and physical activity was performed by comparing the MA dataset with the GESTALT dataset. The details of the GESTALT dataset is available on PRIDE repository PXD011967, and GESTALT subject characteristics are provided in Figure 5-figure supplement 1.

4.9 Statistical analyses

Statistical comparisons of physical function tests, thigh cross-sectional area, mtDNA copy number, and protein abundance by Western blot (VDAC) were performed using a two-tailed Student's t-test, with $P<0.05$. Statistical comparison of fiber type proportion, fiber size by type, Western blot (oxphos complex subunit abundance), and the abundance of respiratory chain compromised fibers was performed by Two-Way ANOVA, with a Sidak multiple comparison posthoc test.

For LCMS analyses, protein significance was determined with p-values derived from one-way analysis of variance test to check any possible statistically significant difference between groups. The *p* value threshold for a protein was considered as significant if $p<0.05$. Partial Least Square analysis (PLS) was used to derive models with the classification that maximized the variance between MA and NA groups. PLS loadings were derived from log2 normalized protein reporter ion intensity from all proteins. The statistical method was performed using R 3.3.6 with inbuilt libraries. Heat maps and hierarchical cluster analyses were performed using the non-linear minimization package in R. GraphPad PRISM 6.07, and R Bioconductor packages were used for statistical analysis and generation of figures. STRING analysis (Szklarczyk *et al.*, 2019) was used for obtaining protein-protein interaction network. Enrichment analysis was performed by ClueGO (Bindea *et al.*, 2009) and PANTHER; the pathways were mapped and visualized by Cytoscape 3.7.2. One-way ANOVA, nonparametric, and chi-square tests (continuous and categorical variables) were used to test for sample differences.

TABLE LEGENDS

Table 1. Characteristics of NA and MA.

Table 2. Training and competition history of octogenarian MA.

FIGURE LEGENDS

Figure 1. (a-f) Clinical function tests in NA and MA. (g) Thigh cross sectional image of an 80 y old male NA (h) and an 83 y old male MA. (i) The total cross-sectional area (CSA) of the thigh/height was greater in MA than NA. (j) Maximal isokinetic strength during knee extension was greater in MA than NA. Graphs show means and standard deviations. Groups were compared by a two-tailed Student's t-test, with $P<0.05$.

Figure 2. The quantitative proteome reveals temporal proteome changes between MA and NA. (a) Number of proteins quantified among 3 TMT batches. (b) Quantitative protein expression between 3 TMT batches. (c) PLS plot of MA and NA donors. Red circles are MA donors and cyan circles are NA donors. (d) Proteins differentially expressed between MA and NA. Each circle is a protein, red circles are proteins increased in abundance in MA, and blue circles are proteins decreased in abundance in MA. (e) Cellular location of the differentially expressed proteins in MA and the number of proteins encoded for each component is shown (X-axis).

Figure 3. Mitochondrial protein enrichment in octogenarian MA. (a) Dysregulation of significant mitochondrial proteins shown as red circles. (b) Functional classification of mitochondrial proteins with protein-protein interaction enrichment p-value < 1.0e-16. (c) Heatmap showing upregulated respiratory chain complex proteins in MA. 71 complex proteins on y-axis. X-axis shows donors. (d) Enrichment of mitochondrial sirtuins SIRT5 and SIRT3 in muscle of MA versus NA. (e) Respiratory chain compromised fibers in skeletal muscle. COX/SDH image showing the identification of COXPos (brown cells), COXInt (empty stars), and COXneg muscle fibers (solid star). COXNeg fibers have lost complex IV activity and appear blue, COXInt retain small amounts of COX activity and appear grey, and COXPos fibers have normal COX function and appear brown. Scale = 200 μm. (f) Quantification revealed a significantly higher abundance of healthy COXPos fibers (*p=0.0291) and fewer respiratory chain compromised (COXInt) myofibers (*p=0.0448) in MA compared to NA. (g) Upregulation of mtDNA in MA. MA and NA donors are shown on X-axis; quantified mtDNA proteins are shown on Y axis. (h) Increased mtDNA copy number in MAs. Absolute mtDNA copy number was determined using a standard curve constructed from known amounts of mtDNA. MA had significantly more copies of mtDNA than NA (*p=0.0177; t-test). Graph shows the means and standard deviation. (i) Protein groups that maintain the functional integrity of mitochondria were higher in MA. (j) Upregulated MA proteins in MICOS complex system and the fold change of the proteins. Cellular location of the proteins is color coded.

736 **Figure 4.** Dysregulation of spliceosome pathway proteins in octogenarian MA. (a)
737 Underrepresentation of spliceosome pathway proteins. Significant spliceosome proteins (22)
738 underrepresented in MA are marked as red circles and all other proteins are marked as grey
739 circle. X-axis shows log2 fold expression of the proteins in MA versus NA. (b) The functional
740 characteristics of the spliceosome proteins are shown. Each GO annotation cluster is color
741 coded. (c) Down-regulation of TRA2 protein in MA donors. Y-axis shows the log2 relative
742 protein abundance. (d) Interaction partners of TRA2 protein; with RNA splicing regulation
743 proteins, mRNA major splicing pathway, and mRNA minor splicing pathway proteins.

744 **Figure 5.** Proteins that decline with aging but are antagonized in physically active subjects
745 (GESTALT, n=58) and MA group. Enriched pathways from 50 proteins which increase with PA
746 and MA and decrease with Age are shown (top), pathways from 12 proteins which are in
747 common between PA and Age (left) and enriched pathways from 22 proteins which are in
748 common between MA and Age (right). Top enriched pathways are color coded (significance
749 threshold FDR <0.05). Proteins without interaction partners are omitted from visualization.

750 **Figure 6:** MA exclusive over-represented proteins. The subset of 301 MA+ proteome
751 represents cluster of mitochondrial translation pathway enrichment (blue circles, 36 proteins),
752 mitochondrial inner membrane (red circles, 75 proteins) and mitochondrial matrix proteins (pink,
753 65 proteins). Mitochondrial translation pathway proteins are localized either as inner membrane
754 proteins or as matrix proteins. Each circle node is a protein exclusive to MA from (MA+, PA+
755 and Age-) analysis, Nodes without any interaction are excluded from the enrichment analysis.

756 **Figure 7:** MA exclusive under-represented proteins. (a) Proteins that increase with aging but
757 are antagonized in physically active subjects (GESTALT, n=58) and MA group. Enriched
758 pathways from 40 proteins which decrease with PA and MA and increase with Age are shown
759 (top), pathways from 141 proteins which are in common between PA and Age (left) and
760 enriched pathways from 80 proteins which are in common between MA and Age (right) are
761 shown. Network analysis and enrichment analysis are performed using STRING analysis tool;
762 the top enriched pathways are color coded (p <0.05). Proteins without interaction partners are
763 omitted from visualization. (b) The subset of 162 MA- proteome represents cluster of chromatin
764 organization, nuclear pore, mRNA splicing process and contractile fiber proteins. This cluster of
765 proteins appear unrelated to physical activity and may reflect unique biology in MA group.
766 Protein protein interaction pathways and GO cellular components shown here are significantly
767 enriched (p< 1.0e-16).

768

769 **ACKNOWLEDGMENTS**

770 We thank the Master Athlete study participants and the GESTALT participants. We thank
771 Lauren Brick for assistance with figure design. Funding for this study was provided by operating
772 grants from the Canadian Institutes of Health Research (MOP 84408 to TT and MOP 125986 to
773 RTH). Supported in part by the Intramural Research Program of the National Institute on Aging,
774 NIH, Baltimore, MD, United States.

775 **CONFLICT OF INTEREST**

776 The authors declare no conflict of interest.

777 **AUTHOR CONTRIBUTIONS**

778 LF, TT and RH designed the research. TT and JM collected the muscle biopsies and SS
779 performed mtDNA experiments. SS, NM, and MF performed phenotypical analysis of the data.
780 CU, AL designed the mass spectrometry experiment and AL generated the data. CU, LF, RH
781 performed the data analysis, prepared the figures, and analyzed the data**.** All authors wrote the
782 manuscript and gave final approval for publication.

783 **DATA AVAILABILITY**

784 The mass spectrometry proteomics data have been deposited to the MassIVE with the dataset
785 identifier MSV000086195 (ftp://MSV000086195@massive.ucsd.edu), reviewer user name (
786 MSV000086195_reviewer).

787

REFERENCES

Adelnia, F., Ubaida-Mohien, C., Moaddel, R., Shardell, M., Lyashkov, A., Fishbein, K. W., . . . Ferrucci, L. (2020). Proteomic signatures of in vivo muscle oxidative capacity in healthy adults. *Aging Cell, 19*(4), e13124. doi:10.1111/acel.13124

Ahn, B. H., Kim, H. S., Song, S., Lee, I. H., Liu, J., Vassilopoulos, A., . . . Finkel, T. (2008). A role for the mitochondrial deacetylase Sirt3 in regulating energy homeostasis. *Proc Natl Acad Sci U S A, 105*(38), 14447-14452. doi:10.1073/pnas.0803790105

Bess, A. S., Crocker, T. L., Ryde, I. T., & Meyer, J. N. (2012). Mitochondrial dynamics and autophagy aid in removal of persistent mitochondrial DNA damage in Caenorhabditis elegans. *Nucleic Acids Res, 40*(16), 7916-7931. doi:10.1093/nar/gks532

Bhadra, M., Howell, P., Dutta, S., Heintz, C., & Mair, W. B. (2020). Alternative splicing in aging and longevity. *Hum Genet, 139*(3), 357-369. doi:10.1007/s00439-019-02094-6

Bindea, G., Mlecnik, B., Hackl, H., Charoentong, P., Tosolini, M., Kirilovsky, A., . . . Galon, J. (2009). ClueGO: a Cytoscape plug-in to decipher functionally grouped gene ontology and pathway annotation networks. *Bioinformatics, 25*(8), 1091-1093. doi:10.1093/bioinformatics/btp101

Brandauer, J., Andersen, M. A., Kellezi, H., Risis, S., Frosig, C., Vienberg, S. G., & Treebak, J. T. (2015). AMP-activated protein kinase controls exercise training- and AICAR-induced increases in SIRT3 and MnSOD. *Front Physiol, 6*, 85. doi:10.3389/fphys.2015.00085

Bua, E., Johnson, J., Herbst, A., Delong, B., McKenzie, D., Salamat, S., & Aiken, J. M. (2006). Mitochondrial DNA-deletion mutations accumulate intracellularly to detrimental levels in aged human skeletal muscle fibers. *Am J Hum.Genet., 79*(3), 469-480.

Cawthon, P. M., Travison, T. G., Manini, T. M., Patel, S., Pencina, K. M., Fielding, R. A., . . . Outcomes Consortium Conference, p. (2019). Establishing the Link Between Lean Mass and Grip Strength Cut-points With Mobility Disability and Other Health Outcomes: Proceedings of the Sarcopenia Definition and Outcomes Consortium Conference. *J Gerontol A Biol Sci Med Sci*. doi:10.1093/gerona/glz081

Cho, Y., Hazen, B. C., Gandra, P. G., Ward, S. R., Schenk, S., Russell, A. P., & Kralli, A. (2016). Perm1 enhances mitochondrial biogenesis, oxidative capacity, and fatigue resistance in adult skeletal muscle. *FASEB J, 30*(2), 674-687. doi:10.1096/fj.15-276360

Cimen, H., Han, M. J., Yang, Y., Tong, Q., Koc, H., & Koc, E. C. (2010). Regulation of succinate dehydrogenase activity by SIRT3 in mammalian mitochondria. *Biochemistry, 49*(2), 304-311. doi:10.1021/bi901627u

Cogliati, S., Frezza, C., Soriano, M. E., Varanita, T., Quintana-Cabrera, R., Corrado, M., . . . Scorrano, L. (2013). Mitochondrial cristae shape determines respiratory chain supercomplexes assembly and respiratory efficiency. *Cell, 155*(1), 160-171. doi:10.1016/j.cell.2013.08.032

Deschenes, M., & Chabot, B. (2017). The emerging role of alternative splicing in senescence and aging. *Aging Cell, 16*(5), 918-933. doi:10.1111/acel.12646

Dulac, M., Leduc-Gaudet, J. P., Reynaud, O., Ayoub, M. B., Guerin, A., Finkelchtein, M., . . . Gouspillou, G. (2020). Drp1 knockdown induces severe muscle atrophy and remodelling, mitochondrial dysfunction, autophagy impairment and denervation. *J Physiol, 598*(17), 3691-3710. doi:10.1113/JP279802

Gao, L., Kumar, V., Vellichirammal, N. N., Park, S. Y., Rudebush, T. L., Yu, L., . . . Zucker, I. H. (2020). Functional, proteomic and bioinformatic analyses of Nrf2- and Keap1- null skeletal muscle. *J Physiol*. doi:10.1113/JP280176

Goodpaster, B. H., Park, S. W., Harris, T. B., Kritchevsky, S. B., Nevitt, M., Schwartz, A. V., . . . Newman, A. B. (2006). The loss of skeletal muscle strength, mass, and quality in older adults: the health, aging and body composition study. *J Gerontol A Biol Sci Med Sci, 61*(10), 1059-1064.

835 Gram, M., Vigelso, A., Yokota, T., Helge, J. W., Dela, F., & Hey-Mogensen, M. (2015). Skeletal muscle
836 mitochondrial H2 O2 emission increases with immobilization and decreases after aerobic
837 training in young and older men. *J Physiol, 593*(17), 4011-4027. doi:10.1113/JP270211
838 Greaves, L. C., Yu-Wai-Man, P., Blakely, E. L., Krishnan, K. J., Beadle, N. E., Kerin, J., . . . Taylor, R. W.
839 (2010). Mitochondrial DNA defects and selective extraocular muscle involvement in CPEO. *Invest*
840 *Ophthalmol Vis Sci, 51*(7), 3340-3346. doi:10.1167/iovs.09-4659
841 Harries, L. W., Hernandez, D., Henley, W., Wood, A. R., Holly, A. C., Bradley-Smith, R. M., . . . Melzer, D.
842 (2011). Human aging is characterized by focused changes in gene expression and deregulation of
843 alternative splicing. *Aging Cell, 10*(5), 868-878. doi:10.1111/j.1474-9726.2011.00726.x
844 Hepple, R. T. (2016). Impact of aging on mitochondrial function in cardiac and skeletal muscle. *Free*
845 *Radic Biol Med, 98*, 177-186. doi:10.1016/j.freeradbiomed.2016.03.017
846 Herbrich, S. M., Cole, R. N., West, K. P., Jr., Schulze, K., Yager, J. D., Groopman, J. D., . . . Ruczinski, I.
847 (2013). Statistical inference from multiple iTRAQ experiments without using common reference
848 standards. *J Proteome Res, 12*(2), 594-604. doi:10.1021/pr300624g
849 Hinkley, J. M., Cornnell, H. H., Standley, R. A., Chen, E. Y., Narain, N. R., Greenwood, B. P., . . . Coen, P. M.
850 (2020). Older adults with sarcopenia have distinct skeletal muscle phosphodiester,
851 phosphocreatine, and phospholipid profiles. *Aging Cell, 19*(6), e13135. doi:10.1111/acel.13135
852 Holly, A. C., Melzer, D., Pilling, L. C., Fellows, A. C., Tanaka, T., Ferrucci, L., & Harries, L. W. (2013).
853 Changes in splicing factor expression are associated with advancing age in man. *Mech Ageing*
854 *Dev, 134*(9), 356-366. doi:10.1016/j.mad.2013.05.006
855 Hood, D. A., Memme, J. M., Oliveira, A. N., & Triolo, M. (2019). Maintenance of Skeletal Muscle
856 Mitochondria in Health, Exercise, and Aging. *Annu Rev Physiol, 81*, 19-41. doi:10.1146/annurev-
857 physiol-020518-114310
858 Huynen, M. A., Muhlmeister, M., Gotthardt, K., Guerrero-Castillo, S., & Brandt, U. (2016). Evolution and
859 structural organization of the mitochondrial contact site (MICOS) complex and the
860 mitochondrial intermembrane space bridging (MIB) complex. *Biochim Biophys Acta, 1863*(1), 91-
861 101. doi:10.1016/j.bbamcr.2015.10.009
862 John, G. B., Shang, Y., Li, L., Renken, C., Mannella, C. A., Selker, J. M., . . . Zha, J. (2005). The
863 mitochondrial inner membrane protein mitofilin controls cristae morphology. *Mol Biol Cell,*
864 *16*(3), 1543-1554. doi:10.1091/mbc.e04-08-0697
865 Kammers, K., Cole, R. N., Tiengwe, C., & Ruczinski, I. (2015). Detecting Significant Changes in Protein
866 Abundance. *EuPA Open Proteom, 7*, 11-19. doi:10.1016/j.euprot.2015.02.002
867 Kleinert, M., Parker, B. L., Jensen, T. E., Raun, S. H., Pham, P., Han, X., . . . Sylow, L. (2018). Quantitative
868 proteomic characterization of cellular pathways associated with altered insulin sensitivity in
869 skeletal muscle following high-fat diet feeding and exercise training. *Sci Rep, 8*(1), 10723.
870 doi:10.1038/s41598-018-28540-5
871 Koltai, E., Bori, Z., Osvath, P., Ihasz, F., Peter, S., Toth, G., . . . Radak, Z. (2018). Master athletes have
872 higher miR-7, SIRT3 and SOD2 expression in skeletal muscle than age-matched sedentary
873 controls. *Redox Biol, 19*, 46-51. doi:10.1016/j.redox.2018.07.022
874 Lindenboim, L., Zohar, H., Worman, H. J., & Stein, R. (2020). The nuclear envelope: target and mediator
875 of the apoptotic process. *Cell Death Discov, 6*, 29. doi:10.1038/s41420-020-0256-5
876 Mishra, P., Carelli, V., Manfredi, G., & Chan, D. C. (2014). Proteolytic cleavage of Opa1 stimulates
877 mitochondrial inner membrane fusion and couples fusion to oxidative phosphorylation. *Cell*
878 *Metab, 19*(4), 630-641. doi:10.1016/j.cmet.2014.03.011
879 Mounier, R., Theret, M., Lantier, L., Foretz, M., & Viollet, B. (2015). Expanding roles for AMPK in skeletal
880 muscle plasticity. *Trends Endocrinol Metab, 26*(6), 275-286. doi:10.1016/j.tem.2015.02.009
881 Mueller, E. E., Mayr, J. A., Zimmermann, F. A., Feichtinger, R. G., Stanger, O., Sperl, W., & Kofler, B.
882 (2012). Reduction of nuclear encoded enzymes of mitochondrial energy metabolism in cells

devoid of mitochondrial DNA. *Biochemical and Biophysical Research Communications, 417*(3), 1052-1057. doi:10.1016/j.bbrc.2011.12.093

Muller-Hocker, J., Seibel, P., Schneiderbanger, K., & Kadenbach, B. (1993). Different in situ hybridization patterns of mitochondrial DNA in cytochrome c oxidase-deficient extraocular muscle fibres in the elderly. *Virchows Arch.A Pathol.Anat.Histopathol., 422*(1), 7-15.

Murphy, J. L., Ratnaike, T. E., Shang, E., Falkous, G., Blakely, E. L., Alston, C. L., . . . Turnbull, D. M. (2012). Cytochrome c oxidase-intermediate fibres: importance in understanding the pathogenesis and treatment of mitochondrial myopathy. *Neuromuscul Disord, 22*(8), 690-698. doi:10.1016/j.nmd.2012.04.003

Nilsson, M. I., & Tarnopolsky, M. A. (2019). Mitochondria and Aging-The Role of Exercise as a Countermeasure. *Biology (Basel), 8*(2). doi:10.3390/biology8020040

Old, S. L., & Johnson, M. A. (1989). Methods of microphotometric assay of succinate dehydrogenase and cytochrome c oxidase activities for use on human skeletal muscle. *Histochemical Journal, 21*, 545-555.

Ott, C., Ross, K., Straub, S., Thiede, B., Gotz, M., Goosmann, C., . . . Kozjak-Pavlovic, V. (2012). Sam50 functions in mitochondrial intermembrane space bridging and biogenesis of respiratory complexes. *Mol Cell Biol, 32*(6), 1173-1188. doi:10.1128/MCB.06388-11

Pereira, C. A., Carlos, D., Ferreira, N. S., Silva, J. F., Zanotto, C. Z., Zamboni, D. S., . . . Tostes, R. C. (2019). Mitochondrial DNA Promotes NLRP3 Inflammasome Activation and Contributes to Endothelial Dysfunction and Inflammation in Type 1 Diabetes. *Front Physiol, 10*, 1557. doi:10.3389/fphys.2019.01557

Power, G. A., Allen, M. D., Gilmore, K. J., Stashuk, D. W., Doherty, T. J., Hepple, R. T., . . . Rice, C. L. (2016). Motor unit number and transmission stability in octogenarian world class athletes: Can age-related deficits be outrun? *J Appl Physiol (1985), 121*(4), 1013-1020. doi:10.1152/japplphysiol.00149.2016

Qi, Y., Kapterian, T. S., Du, X., Ma, Q., Fei, W., Zhang, Y., . . . Yang, H. (2016). CDP-diacylglycerol synthases regulate the growth of lipid droplets and adipocyte development. *J Lipid Res, 57*(5), 767-780. doi:10.1194/jlr.M060574

Rodriguez, S. A., Grochova, D., McKenna, T., Borate, B., Trivedi, N. S., Erdos, M. R., & Eriksson, M. (2016). Global genome splicing analysis reveals an increased number of alternatively spliced genes with aging. *Aging Cell, 15*(2), 267-278. doi:10.1111/acel.12433

Sonjak, V., Jacob, K., Morais, J. A., Rivera-Zengotita, M., Spendiff, S., Spake, C., . . . Hepple, R. T. (2019). Fidelity of muscle fibre reinnervation modulates ageing muscle impact in elderly women. *J Physiol, 597*(19), 5009-5023. doi:10.1113/JP278261

Spendiff, S., Vuda, M., Gouspillou, G., Aare, S., Perez, A., Morais, J. A., . . . Hepple, R. T. (2016). Denervation drives mitochondrial dysfunction in skeletal muscle of octogenarians. *J Physiol, 594*(24), 7361-7379. doi:10.1113/JP272487

Stewart, M. (2019). Polyadenylation and nuclear export of mRNAs. *J Biol Chem, 294*(9), 2977-2987. doi:10.1074/jbc.REV118.005594

Strambio-De-Castillia, C., Niepel, M., & Rout, M. P. (2010). The nuclear pore complex: bridging nuclear transport and gene regulation. *Nat Rev Mol Cell Biol, 11*(7), 490-501. doi:10.1038/nrm2928

Szklarczyk, D., Gable, A. L., Lyon, D., Junge, A., Wyder, S., Huerta-Cepas, J., . . . Mering, C. V. (2019). STRING v11: protein-protein association networks with increased coverage, supporting functional discovery in genome-wide experimental datasets. *Nucleic Acids Res, 47*(D1), D607-D613. doi:10.1093/nar/gky1131

Tao, R., Coleman, M. C., Pennington, J. D., Ozden, O., Park, S. H., Jiang, H., . . . Gius, D. (2010). Sirt3-mediated deacetylation of evolutionarily conserved lysine 122 regulates MnSOD activity in response to stress. *Mol Cell, 40*(6), 893-904. doi:10.1016/j.molcel.2010.12.013

Taylor, R. W., Barron, M. J., Borthwick, G. M., Gospel, A., Chinnery, P. F., Samuels, D. C., . . . Turnbull, D. M. (2003). Mitochondrial DNA mutations in human colonic crypt stem cells. *Journal of Clinical Investigation, 112*(9), 1351-1360.

Tezze, C., Romanello, V., Desbats, M. A., Fadini, G. P., Albiero, M., Favaro, G., . . . Sandri, M. (2017). Age-Associated Loss of OPA1 in Muscle Impacts Muscle Mass, Metabolic Homeostasis, Systemic Inflammation, and Epithelial Senescence. *Cell Metab, 25*(6), 1374-1389 e1376. doi:10.1016/j.cmet.2017.04.021

Ubaida-Mohien, C., Gonzalez-Freire, M., Lyashkov, A., Moaddel, R., Chia, C. W., Simonsick, E. M., . . . Ferrucci, L. (2019). Physical Activity Associated Proteomics of Skeletal Muscle: Being Physically Active in Daily Life May Protect Skeletal Muscle From Aging. *Front Physiol, 10*, 312. doi:10.3389/fphys.2019.00312

Ubaida-Mohien, C., Lyashkov, A., Gonzalez-Freire, M., Tharakan, R., Shardell, M., Moaddel, R., . . . Ferrucci, L. (2019). Discovery proteomics in aging human skeletal muscle finds change in spliceosome, immunity, proteostasis and mitochondria. *Elife, 8*. doi:10.7554/eLife.49874

Wente, S. R., & Rout, M. P. (2010). The nuclear pore complex and nuclear transport. *Cold Spring Harb Perspect Biol, 2*(10), a000562. doi:10.1101/cshperspect.a000562

Wisniewski, J. R., Zougman, A., Nagaraj, N., & Mann, M. (2009). Universal sample preparation method for proteome analysis. *Nat Methods, 6*(5), 359-362. doi:10.1038/nmeth.1322

SUPPLEMENTARY METHOD, FIGURES

Supplemental Method

4.4 Histochemical labeling for respiratory compromised muscle fibers

COX/SDH histochemistry (Old & Johnson, 1989; Taylor *et al.*, 2003) was performed to assess the activity of OXPHOS complexes IV (COX) and II (SDH), and thus identify muscle fibers with a respiratory chain deficiency (COX^{Neg}). The COX incubation medium was prepared by adding 100 µM cytochrome *c* to 4 mM of 3,3-diaminobenzidine tetrahydrochloride (DAB) with 20 µg of catalase. The slides were incubated for 45 minutes at 37°C in a humidified chamber. Following three washes in phosphate-buffered saline (PBS), SDH incubation medium (130 mM sodium succinate, 200 µM phenazine methosulphate, 1 mM sodium azide, and 1.5 mM NitroBlue tetrazolium) was added to the sections. The sections were again incubated for 45 minutes at 37°C, washed x3 PBS, and then dehydrated through a graded ethanol series and xylene before being mounted in DPX. Images of the whole muscle section were captured on a Zeiss Axio Imager M2 fluorescent microscope (Zeiss, Germany). Counts of COX positive (COX^{Pos}), COX^{Int}, and COX^{Neg} myofibers were performed for the whole muscle cross-section. COX negative fibers are indicative of cells with high levels of mtDNA mutations (Bua *et al.*, 2006a; Murphy *et al.*, 2012b) and will thus not demonstrate the brown reaction product (oxidized DAB) during the first

incubation but will stain blue following the second incubation for SDH activity. This is because the nuclear DNA entirely encodes SDH, so any mtDNA mutations will not affect its activity. In contrast, mtDNA mutations could affect complex IV activity and prevent DAB oxidation if a mutation affects a region of mtDNA containing the Cox subunit genes.

4.5 Mitochondrial DNA copy number

Groups of 25 fibers (5 x 5 fibers) in an unstained 20-μm thick muscle cross-section were randomly selected (random number generator & numbered grid), laser captured, and their DNA extracted using the lysis method (Spendiff *et al.*, 2013) and stored at -20oC. The products were then separated on a 1% agarose gel containing Sybr® Safe DNA Gel Stain at 70 V for 30 mins, and the bands visualized using a G-Box chem imaging system (Figure 1–figure supplement 1a). The mtDNA fragment was extracted using a QiAquick Gel Extraction Kit and quantified using a NanoDrop-2000 spectrophotometer (Thermo scientific). Total mtDNA copy number in muscle fibers was determined using a standard curve created from the amplification of MTND1 (1011bp fragment, forward primer: 5' TGTAAAACGACGGCCAGT 3', reverse primer: 5' CAGGAAACAGCTATGACC) (Greaves *et al.*, 2010) (Figure 1–figure supplement 1b). The products were separated on a 1% agarose gel, and the mtDNA fragment extracted using a QiAquick Gel Extraction Kit and quantified with a NanoDrop-2000 spectrophotometer (Thermo scientific). A standard curve was generated by serially diluting down the sample in dH2O. Groups of 25 fibres (5 x 5 fibres) were randomly selected (random number generator & numbered grid) and laser captured. Samples along with the standard curve were run in triplicate using an MTND1 TaqMan® qPCR assay (Forward primer: 5' CCCTAAAACCCGCCACATCT 3', reverse primer: 5' GAGCGATGGTGAGAGCTAAGGT 3', probe: 5' VIC- CCATCACCCTCTACATCACCGCCC 3'). The total mtDNA copy number was then determined using the sample Cq values and the equation generated from the standard curve. Results were divided by the total area of the captured cells to give mtDNA copy number per area.

4.6 Western blotting for mitochondrial proteins

Western blotting for representative mitochondrial proteins was performed as previously (Spendiff *et al.*, 2016). Briefly, 10-20 mg of muscle was homogenized in a Retch mixer mill (MM400) with 10 x (w/v) of extraction buffer (50 mM Tris base, 150 mM NaCl, 1% Triton X-100, 0.5% sodium deoxycolate, 0.1% sodium dodecyl sulphate, and 10 ul per ml of Protease Inhibitor

Cocktail. Following 2 h of gentel agitation at 4C, samples were centrifuged at 12,000 g for 20 min at 4C, and the supernatant removed for protein assessment by Bradford assay. Samples were diluted in 4 x Laemli buffer to yield a final protein concentration of 2 ug per ml and then boiled for 5 min at 95C. Immunoblotting was done using 20 ug of protein, loaded onto a 12% acrylamide gel, electrophoresed by SDS-PAGE and then transferred to polyvinylidene fluoride membranes (Life Sciences), blocked for 1 h at room temperature in 5% (w/v) semi-skinned milk, and probed overnight at 4C with the following primary antibodies (diluted in 5% BSA): mouse monoclonal anti-VDAC (1:1000; Abcam ab14734), and mouse monoclonal Total OXPHOS Cocktail (1:2000, Abcam ab110413). To address the poorer sensitivity to the CIV subunit in this cocktail after boiling human samples, we also probed using mouse monoclonal CIV (1:1000, Life Technologies A21348). Ponceau staining was performed to normalize protein loading. Following washing, membranes were incubated with HRP-conjugated secondary antibodies (diluted in 5% milk, Abcam) for 1 h at room temperature. Protein bands were detected using SuperSignal™ West Pico Chemiluminescent Substrate (Thermo Scientific, USA) and imaged with a G-Box Chem Imaging System. Analysis of protein bands was performed using GeneTools software (Syngenem, UK).

4.7 Sample preparation and protein extraction for MS

Roughly, 5 to 8 mg of vastus lateralis muscle tissue was pulverized in liquid nitrogen and mixed with the modified SDT lysis buffer (100 mM Tris, 140 mM NaCl, 4% SDS, 1% Triton X-114, pH 7.6 (Sigma)) (Wisniewski *et al.*, 2009). Tissues were sonicated using preprogramed tabletop tip sonicator, centrifuged at +4°C for 15 min at 14000 rpm, aliquoted, and stored at -80°C until further processing. Protein concentration was determined using a commercially available 2-D quant kit (GE Healthcare Life Sciences). The sample quality was confirmed using NuPAGE® protein gels stained with fluorescent SyproRuby protein stain (Thermo Fisher). 300 µg of muscle tissue lysate was used for tryptic digestion.

Detergents and lipids were removed by standard methanol/chloroform extraction protocol (sample:methanol:chloroform:water – 1:4:1:3) (Wessel & Flugge, 1984). Purified proteins were resuspended using a small aliquot (30 µl) of concentrated urea buffer (8M Urea, 2M Thiourea, 150 mM NaCl (Sigma)), reduced with 50 mM DTT for 1 hour at 36°C and alkylated with 100 mM iodoacetamide for 1 hour at 36°C in the dark. Concentrated urea was diluted 12 times with 50 mM ammonium bicarbonate buffer. Proteins were digested for 18 hours at 36°C using trypsin/LysC mixture (Promega) in 1:50 (w/w) enzyme to protein ratio. Protein digests were

desalted on 10 x 4.0 mm C18 cartridge using Agilent 1260 Bio-inert HPLC system connected to the fraction collector. Purified peptides were speed vacuum dried and stored at -80°C.

Initially, three independent 10-plex tandem mass spectrometry tag (TMT 10-plex) experiments were designed. Samples in each TMT experiment were blinded and randomized between TMT channels to avoid labeling and sampling bias. Each LC-MS experiment used 100 µg of muscle tissue digest from 5 MA samples matched with 5 controls (NA) that were independently labeled with 10-plex tags (Thermo Fisher). Of the three 10-plex experiment, a total of 24 biological replicates and 6 technical replicates were included, technical replicates were used to optimize instrument performane and to estimate technical reproducibilty. 200 femtomole of bacterial beta-galactosidase digest (SCIEX) was spiked into each sample prior to TMT labeling to control labeling efficiency and overall instrument performance. Labeled peptides were combined into one experiment and fractionated.

4.8 High-pH RPLC fractionation and concatenation strategy

Basic reverse phase fractionation was done on Agilent 1260 bioinert HPLC system as previously described (Wang *et al.*, 2011). XBridge 4.6 mm X 250 mm column (Peptide BEH C18) equipped with 3.9 mm X 5 mm XBridge BEH Shield RP18 XP VanGuard cartridge (Waters). The solvent composition was as follows: 10mM ammonium formate (pH 10) as mobile phase (A) and 10mM ammonium formate and 90% ACN (pH 10) as mobile-phase B. Labeled peptides were separated using a linear organic gradient (5% to 50% B in 100 min). Initially, 99 fractions were collected during each LC run at 1 min intervals each. Three fractions separated by 33 min intervals were concatenated into 33 master fractions, as previously described (Ubaida-Mohien *et al.*, 2019a).

4.9 nano LC-MS/MS analyses

Purified peptide fractions from muscle tissues were analyzed using UltiMate 3000 Nano LC Systems coupled to the Q Exactive HF mass spectrometer (Thermo Scientific, San Jose, CA). Each fraction was separated on a 45 cm capillary column with 150 □m ID on a linear organic gradient using 550 nl/min flow rate. Gradient went from 5 to 35 %B in 195 min. Mobile phases A and B consisted of 0.1% formic acid in water and 0.1% formic acid in acetonitrile, respectively. Tandem mass spectra were obtained using Q Exactive HF mass spectrometer with the heated capillary temperature +280°C and spray voltage set to 2.5 kV. Full MS1 spectra were acquired from 330 to 1600 m/z at 120000 resolution and 50 ms maximum accumulation time with

automatic gain control [AGC] set to 3x106. Dd-MS2 spectra were acquired using dynamic m/z range with a fixed first mass of 100 m/z. MS/MS spectra were resolved to 30000 with 150 ms of maximum accumulation time and AGC target set to 1x105. Fifteen most abundant ions were selected for fragmentation using 29% normalized high collision energy. A dynamic exclusion time of 70 s was used to discriminate against the previously analyzed ions.

5.0 Proteomics informatics

The PeptideProphet model fits the peptide-spectrum matches into two distributions, one an extreme value distribution for the incorrect matches, and the other a normal distribution for correct matches. The protein was filtered at thresholds of 0.01% peptide FDR, 1% protein FDR and requiring a minimum of 1 unique peptide for protein identification.

Single peptide hits were allowed when any quantifiable peptide was detected across at least 30% of all samples (n=24) and if proteins were identified with more than one search engine. Reporter ion quantitative values were extracted from Scaffold and decoy spectra, contaminant spectra and peptide spectra shared between more than one protein were removed. Typically, spectra are shared between proteins if the two proteins share most of their sequence, usually for protein isoforms. Reporter ions were retained for further analyses if they were exclusive to only one protein, and they were identified in all 10 channels across each TMT batch. Further protein bioinformatics was performed, as previously described (Ubaida-Mohien *et al.*, 2019a)

Extended Method References

Adelnia F, Ubaida-Mohien C, Moaddel R, Shardell M, Lyashkov A, Fishbein KW, Aon MA, Spencer RG & Ferrucci L. (2020). Proteomic signatures of in vivo muscle oxidative capacity in healthy adults. *Aging Cell* **19,** e13124.

Ahn BH, Kim HS, Song S, Lee IH, Liu J, Vassilopoulos A, Deng CX & Finkel T. (2008). A role for the mitochondrial deacetylase Sirt3 in regulating energy homeostasis. *Proc Natl Acad Sci U S A* **105,** 14447-14452.

Bess AS, Crocker TL, Ryde IT & Meyer JN. (2012). Mitochondrial dynamics and autophagy aid in removal of persistent mitochondrial DNA damage in Caenorhabditis elegans. *Nucleic Acids Res* **40,** 7916-7931.

Bhadra M, Howell P, Dutta S, Heintz C & Mair WB. (2020). Alternative splicing in aging and longevity. *Hum Genet* **139,** 357-369.

Bindea G, Mlecnik B, Hackl H, Charoentong P, Tosolini M, Kirilovsky A, Fridman WH, Pages F, Trajanoski Z & Galon J. (2009). ClueGO: a Cytoscape plug-in to decipher functionally grouped gene ontology and pathway annotation networks. *Bioinformatics* **25,** 1091-1093.

Brandauer J, Andersen MA, Kellezi H, Risis S, Frosig C, Vienberg SG & Treebak JT. (2015). AMP-activated protein kinase controls exercise training- and AICAR-induced increases in SIRT3 and MnSOD. *Front Physiol* **6,** 85.

Bua E, Johnson J, Herbst A, Delong B, McKenzie D, Salamat S & Aiken JM. (2006a). Mitochondrial DNA-deletion mutations accumulate intracellularly to detrimental levels in aged human skeletal muscle fibers. *American Journal of Human Genetics* **79,** 469-480.

Bua E, Johnson J, Herbst A, Delong B, McKenzie D, Salamat S & Aiken JM. (2006b). Mitochondrial DNA-deletion mutations accumulate intracellularly to detrimental levels in aged human skeletal muscle fibers. *Am J HumGenet* **79,** 469-480.

Burke SK, Solania A, Wolan DW, Cohen MS, Ryan TE & Hepple RT. (2021). Mitochondrial permeability transition causes mitochondrial reative oxygen species- and caspase 3-dependent atrophy of single adult mouse skeletal muscle fibers. *Cells* **10,** 2586.

Cawthon PM, Travison TG, Manini TM, Patel S, Pencina KM, Fielding RA, Magaziner JM, Newman AB, Brown T, Kiel DP, Cummings SR, Shardel M, Guralnik J, Woodhouse LJ, Pahor M, Binder E, D'Agostino RB, Xue QL, Orwoll E, Landi F, Orwig D, Schaap L, Latham NN, Hirani V, Kwok T, Pereira S, Rooks D, Kashiwa M, Torres-Gonzalez M, Menetski JP, Correa-De-Araujo R, Bhasin S, Sarcopenia D & Outcomes Consortium Conference p. (2019). Establishing the Link Between Lean Mass and Grip Strength Cut-points With Mobility Disability and Other Health Outcomes: Proceedings of the Sarcopenia Definition and Outcomes Consortium Conference. *J Gerontol A Biol Sci Med Sci*.

Cho Y, Hazen BC, Gandra PG, Ward SR, Schenk S, Russell AP & Kralli A. (2016). Perm1 enhances mitochondrial biogenesis, oxidative capacity, and fatigue resistance in adult skeletal muscle. *FASEB J* **30,** 674-687.

Cimen H, Han MJ, Yang Y, Tong Q, Koc H & Koc EC. (2010). Regulation of succinate dehydrogenase activity by SIRT3 in mammalian mitochondria. *Biochemistry* **49,** 304-311.

Cogliati S, Frezza C, Soriano ME, Varanita T, Quintana-Cabrera R, Corrado M, Cipolat S, Costa V, Casarin A, Gomes LC, Perales-Clemente E, Salviati L, Fernandez-Silva P, Enriquez JA & Scorrano L. (2013). Mitochondrial cristae shape determines respiratory chain supercomplexes assembly and respiratory efficiency. *Cell* **155,** 160-171.

Deschenes M & Chabot B. (2017). The emerging role of alternative splicing in senescence and aging. *Aging Cell* **16,** 918-933.

Dulac M, Leduc-Gaudet JP, Reynaud O, Ayoub MB, Guerin A, Finkelchtein M, Hussain SN & Gouspillou G. (2020). Drp1 knockdown induces severe muscle atrophy and remodelling, mitochondrial dysfunction, autophagy impairment and denervation. *J Physiol* **598,** 3691-3710.

Gao L, Kumar V, Vellichirammal NN, Park SY, Rudebush TL, Yu L, Son WM, Pekas EJ, Wafi AM, Hong J, Xiao P, Guda C, Wang HJ, Schultz HD & Zucker IH. (2020). Functional, proteomic and bioinformatic analyses of Nrf2- and Keap1- null skeletal muscle. *J Physiol*.

Goodpaster BH, Park SW, Harris TB, Kritchevsky SB, Nevitt M, Schwartz AV, Simonsick EM, Tylavsky FA, Visser M & Newman AB. (2006). The loss of skeletal muscle strength, mass, and quality in older adults: the health, aging and body composition study. *J Gerontol A Biol Sci Med Sci* **61,** 1059-1064.

Gram M, Vigelso A, Yokota T, Helge JW, Dela F & Hey-Mogensen M. (2015). Skeletal muscle mitochondrial H2 O2 emission increases with immobilization and decreases after aerobic training in young and older men. *J Physiol* **593,** 4011-4027.

Greaves LC, Yu-Wai-Man P, Blakely EL, Krishnan KJ, Beadle NE, Kerin J, Barron MJ, Griffiths PG, Dickinson AJ, Turnbull DM & Taylor RW. (2010). Mitochondrial DNA defects and selective extraocular muscle involvement in CPEO. *Investigative ophthalmology & visual science* **51,** 3340-3346.

Hafner AV, Dai J, Gomes AP, Xiao CY, Palmeira CM, Rosenzweig A & Sinclair DA. (2010). Regulation of the mPTP by SIRT3-mediated deacetylation of CypD at lysine 166 suppresses age-related cardiac hypertrophy. *Aging* **2,** 914-923.

Harries LW, Hernandez D, Henley W, Wood AR, Holly AC, Bradley-Smith RM, Yaghootkar H, Dutta A, Murray A, Frayling TM, Guralnik JM, Bandinelli S, Singleton A, Ferrucci L & Melzer D. (2011). Human aging is characterized by focused changes in gene expression and deregulation of alternative splicing. *Aging Cell* **10,** 868-878.

Hepple RT. (2016). Impact of aging on mitochondrial function in cardiac and skeletal muscle. *Free Radic Biol Med* **98,** 177-186.

Herbrich SM, Cole RN, West KP, Jr., Schulze K, Yager JD, Groopman JD, Christian P, Wu L, O'Meally RN, May DH, McIntosh MW & Ruczinski I. (2013). Statistical inference from multiple iTRAQ experiments without using common reference standards. *J Proteome Res* **12,** 594-604.

Hinkley JM, Cornnell HH, Standley RA, Chen EY, Narain NR, Greenwood BP, Bussberg V, Tolstikov VV, Kiebish MA, Yi F, Vega RB, Goodpaster BH & Coen PM. (2020). Older adults with sarcopenia have distinct skeletal muscle phosphodiester, phosphocreatine, and phospholipid profiles. *Aging Cell* **19,** e13135.

Holly AC, Melzer D, Pilling LC, Fellows AC, Tanaka T, Ferrucci L & Harries LW. (2013). Changes in splicing factor expression are associated with advancing age in man. *Mech Ageing Dev* **134,** 356-366.

Hood DA, Memme JM, Oliveira AN & Triolo M. (2019). Maintenance of Skeletal Muscle Mitochondria in Health, Exercise, and Aging. *Annu Rev Physiol* **81,** 19-41.

Huynen MA, Muhlmeister M, Gotthardt K, Guerrero-Castillo S & Brandt U. (2016). Evolution and structural organization of the mitochondrial contact site (MICOS) complex and the mitochondrial intermembrane space bridging (MIB) complex. *Biochim Biophys Acta* **1863,** 91-101.

John GB, Shang Y, Li L, Renken C, Mannella CA, Selker JM, Rangell L, Bennett MJ & Zha J. (2005). The mitochondrial inner membrane protein mitofilin controls cristae morphology. *Mol Biol Cell* **16,** 1543-1554.

Kammers K, Cole RN, Tiengwe C & Ruczinski I. (2015). Detecting Significant Changes in Protein Abundance. *EuPA Open Proteom* **7,** 11-19.

Kleinert M, Parker BL, Jensen TE, Raun SH, Pham P, Han X, James DE, Richter EA & Sylow L. (2018). Quantitative proteomic characterization of cellular pathways associated with altered insulin sensitivity in skeletal muscle following high-fat diet feeding and exercise training. *Scientific reports* **8,** 10723.

Koltai E, Bori Z, Osvath P, Ihasz F, Peter S, Toth G, Degens H, Rittweger J, Boldogh I & Radak Z. (2018). Master athletes have higher miR-7, SIRT3 and SOD2 expression in skeletal muscle than age-matched sedentary controls. *Redox biology* **19,** 46-51.

Lindenboim L, Zohar H, Worman HJ & Stein R. (2020). The nuclear envelope: target and mediator of the apoptotic process. *Cell Death Discov* **6,** 29.

Mishra P, Carelli V, Manfredi G & Chan DC. (2014). Proteolytic cleavage of Opa1 stimulates mitochondrial inner membrane fusion and couples fusion to oxidative phosphorylation. *Cell Metab* **19,** 630-641.

1215 Mounier R, Theret M, Lantier L, Foretz M & Viollet B. (2015). Expanding roles for AMPK in skeletal
1216 muscle plasticity. *Trends Endocrinol Metab* **26,** 275-286.

1217
1218 Mueller EE, Mayr JA, Zimmermann FA, Feichtinger RG, Stanger O, Sperl W & Kofler B. (2012). Reduction
1219 of nuclear encoded enzymes of mitochondrial energy metabolism in cells devoid of
1220 mitochondrial DNA. *Biochemical and biophysical research communications* **417,** 1052-1057.

1221
1222 Muller-Hocker J, Seibel P, Schneiderbanger K & Kadenbach B. (1993). Different in situ hybridization
1223 patterns of mitochondrial DNA in cytochrome c oxidase-deficient extraocular muscle fibres in
1224 the elderly. *Virchows ArchA PatholAnatHistopathol* **422,** 7-15.

1225
1226 Murphy JL, Ratnaike TE, Shang E, Falkous G, Blakely EL, Alston CL, Taivassalo T, Haller RG, Taylor RW &
1227 Turnbull DM. (2012a). Cytochrome c oxidase-intermediate fibres: importance in understanding
1228 the pathogenesis and treatment of mitochondrial myopathy. *Neuromuscul Disord* **22,** 690-698.

1229
1230 Murphy JL, Ratnaike TE, Shang E, Falkous G, Blakely EL, Alston CL, Taivassalo T, Haller RG, Taylor RW &
1231 Turnbull DM. (2012b). Cytochrome c oxidase-intermediate fibres: Importance in understanding
1232 the pathogenesis and treatment of mitochondrial myopathy. *Neuromuscular Disorders* **22,** 690-
1233 698.

1234
1235 Nilsson MI & Tarnopolsky MA. (2019). Mitochondria and Aging-The Role of Exercise as a
1236 Countermeasure. *Biology (Basel)* **8**.

1237
1238 Old SL & Johnson MA. (1989). Methods of microphotometric assay of succinate dehydrogenase and
1239 cytochrome c oxidase activities for use on human skeletal muscle. *Histochem J* **21,** 545-555.

1240
1241 Ott C, Ross K, Straub S, Thiede B, Gotz M, Goosmann C, Krischke M, Mueller MJ, Krohne G, Rudel T &
1242 Kozjak-Pavlovic V. (2012). Sam50 functions in mitochondrial intermembrane space bridging and
1243 biogenesis of respiratory complexes. *Mol Cell Biol* **32,** 1173-1188.

1244
1245 Pereira CA, Carlos D, Ferreira NS, Silva JF, Zanotto CZ, Zamboni DS, Garcia VD, Ventura DF, Silva JS &
1246 Tostes RC. (2019). Mitochondrial DNA Promotes NLRP3 Inflammasome Activation and
1247 Contributes to Endothelial Dysfunction and Inflammation in Type 1 Diabetes. *Front Physiol* **10,**
1248 1557.

1249
1250 Power GA, Allen MD, Gilmore KJ, Stashuk DW, Doherty TJ, Hepple RT, Taivassalo T & Rice CL. (2016).
1251 Motor unit number and transmission stability in octogenarian world class athletes: Can age-
1252 related deficits be outrun? *J Appl Physiol (1985)* **121,** 1013-1020.

1253

Qi Y, Kapterian TS, Du X, Ma Q, Fei W, Zhang Y, Huang X, Dawes IW & Yang H. (2016). CDP-diacylglycerol synthases regulate the growth of lipid droplets and adipocyte development. *J Lipid Res* **57,** 767-780.

Rodriguez SA, Grochova D, McKenna T, Borate B, Trivedi NS, Erdos MR & Eriksson M. (2016). Global genome splicing analysis reveals an increased number of alternatively spliced genes with aging. *Aging Cell* **15,** 267-278.

Sonjak V, Jacob K, Morais JA, Rivera-Zengotita M, Spendiff S, Spake C, Taivassalo T, Chevalier S & Hepple RT. (2019). Fidelity of muscle fibre reinnervation modulates ageing muscle impact in elderly women. *J Physiol* **597,** 5009-5023.

Spendiff S, Reza M, Murphy JL, Gorman G, Blakely EL, Taylor RW, Horvath R, Campbell G, Newman J, Lochmuller H & Turnbull DM. (2013). Mitochondrial DNA deletions in muscle satellite cells: implications for therapies. *Hum Mol Genet* **22,** 4739-4747.

Spendiff S, Vuda M, Gouspillou G, Aare S, Perez A, Morais JA, Jagoe RT, Filion ME, Glicksman R, Kapchinsky S, MacMillan NJ, Pion CH, Aubertin-Leheudre M, Hettwer S, Correa JA, Taivassalo T & Hepple RT. (2016). Denervation drives mitochondrial dysfunction in skeletal muscle of octogenarians. *J Physiol* **594,** 7361-7379.

Stewart M. (2019). Polyadenylation and nuclear export of mRNAs. *J Biol Chem* **294,** 2977-2987.

Strambio-De-Castillia C, Niepel M & Rout MP. (2010). The nuclear pore complex: bridging nuclear transport and gene regulation. *Nat Rev Mol Cell Biol* **11,** 490-501.

Szklarczyk D, Gable AL, Lyon D, Junge A, Wyder S, Huerta-Cepas J, Simonovic M, Doncheva NT, Morris JH, Bork P, Jensen LJ & Mering CV. (2019). STRING v11: protein-protein association networks with increased coverage, supporting functional discovery in genome-wide experimental datasets. *Nucleic Acids Res* **47,** D607-D613.

Tao R, Coleman MC, Pennington JD, Ozden O, Park SH, Jiang H, Kim HS, Flynn CR, Hill S, Hayes McDonald W, Olivier AK, Spitz DR & Gius D. (2010). Sirt3-mediated deacetylation of evolutionarily conserved lysine 122 regulates MnSOD activity in response to stress. *Mol Cell* **40,** 893-904.

Taylor RW, Barron MJ, Borthwick GM, Gospel A, Chinnery PF, Samuels DC, Taylor GA, Plusa SM, Needham SJ, Greaves LC, Kirkwood TB & Turnbull DM. (2003). Mitochondrial DNA mutations in human colonic crypt stem cells. *Journal of Clinical Investigation* **112,** 1351-1360.

Tezze C, Romanello V, Desbats MA, Fadini GP, Albiero M, Favaro G, Ciciliot S, Soriano ME, Morbidoni V, Cerqua C, Loefler S, Kern H, Franceschi C, Salvioli S, Conte M, Blaauw B, Zampieri S, Salviati L, Scorrano L & Sandri M. (2017). Age-Associated Loss of OPA1 in Muscle Impacts Muscle Mass, Metabolic Homeostasis, Systemic Inflammation, and Epithelial Senescence. *Cell Metab* **25,** 1374-1389 e1376.

Ubaida-Mohien C, Gonzalez-Freire M, Lyashkov A, Moaddel R, Chia CW, Simonsick EM, Sen R & Ferrucci L. (2019a). Physical Activity Associated Proteomics of Skeletal Muscle: Being Physically Active in Daily Life May Protect Skeletal Muscle From Aging. *Front Physiol* **10,** 312.

Ubaida-Mohien C, Lyashkov A, Gonzalez-Freire M, Tharakan R, Shardell M, Moaddel R, Semba RD, Chia CW, Gorospe M, Sen R & Ferrucci L. (2019b). Discovery proteomics in aging human skeletal muscle finds change in spliceosome, immunity, proteostasis and mitochondria. *Elife* **8**.

Wang Y, Yang F, Gritsenko MA, Wang Y, Clauss T, Liu T, Shen Y, Monroe ME, Lopez-Ferrer D, Reno T, Moore RJ, Klemke RL, Camp DG, 2nd & Smith RD. (2011). Reversed-phase chromatography with multiple fraction concatenation strategy for proteome profiling of human MCF10A cells. *Proteomics* **11,** 2019-2026.

Wente SR & Rout MP. (2010). The nuclear pore complex and nuclear transport. *Cold Spring Harb Perspect Biol* **2,** a000562.

Wessel D & Flugge UI. (1984). A method for the quantitative recovery of protein in dilute solution in the presence of detergents and lipids. *Anal Biochem* **138,** 141-143.

Wisniewski JR, Zougman A, Nagaraj N & Mann M. (2009). Universal sample preparation method for proteome analysis. *Nat Methods* **6,** 359-362.

Supplemental Tables & Figures

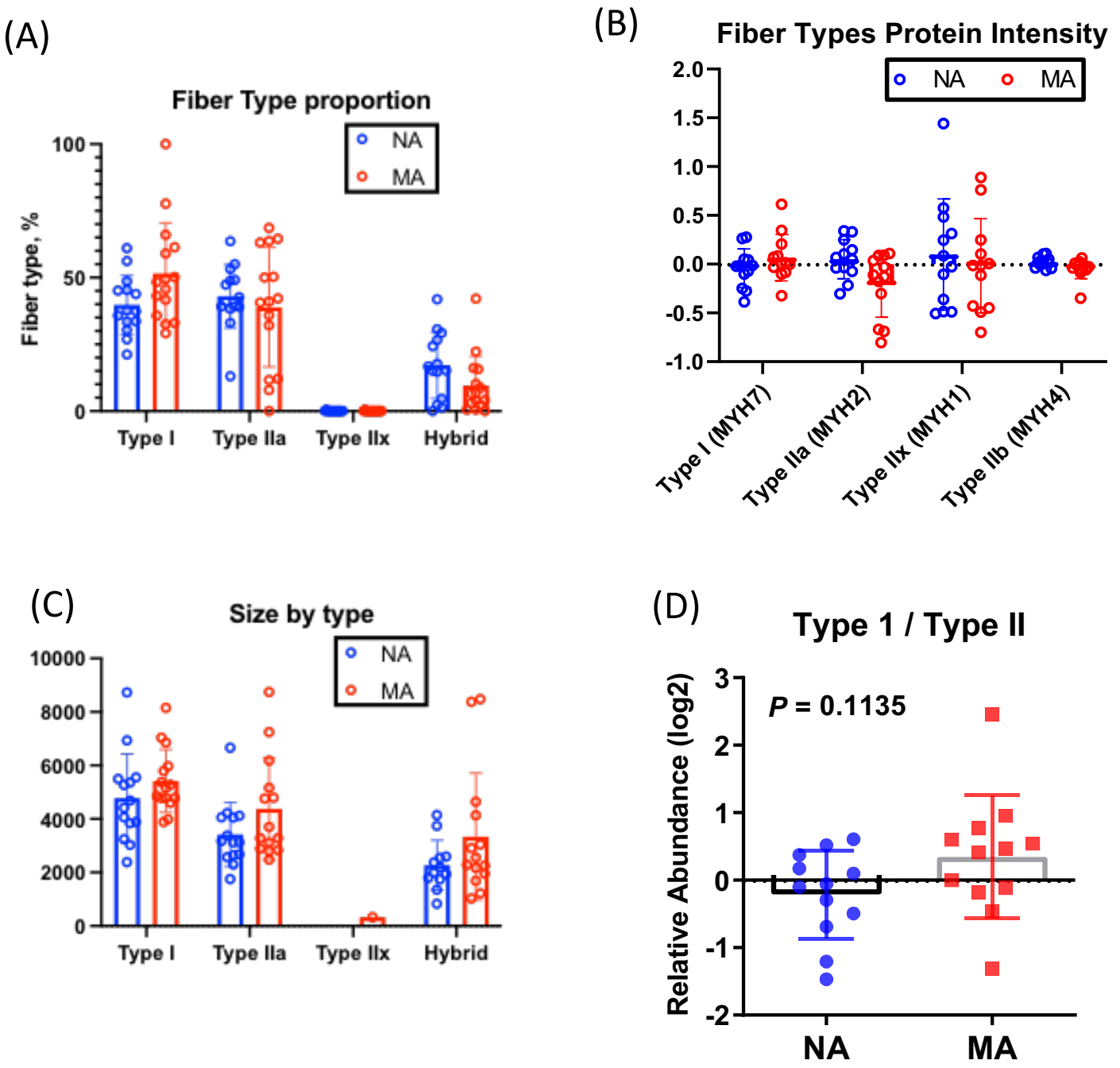

Figure 1-figure supplement 1. (A) Fiber type quantification. Fiber type proportion is quantified using immunofluorescence labelling in NA and MA subjects (left). (**B)** Myosin isoform quantification from the proteomics results from the same subjects (top right), and the ratio of type1 and type 2 fibers (bottom right). **(C)** Fiber size by type and **(D)** type I to type II fiber cross-sectional area ratio from immunolabeled muscle cross-sections.

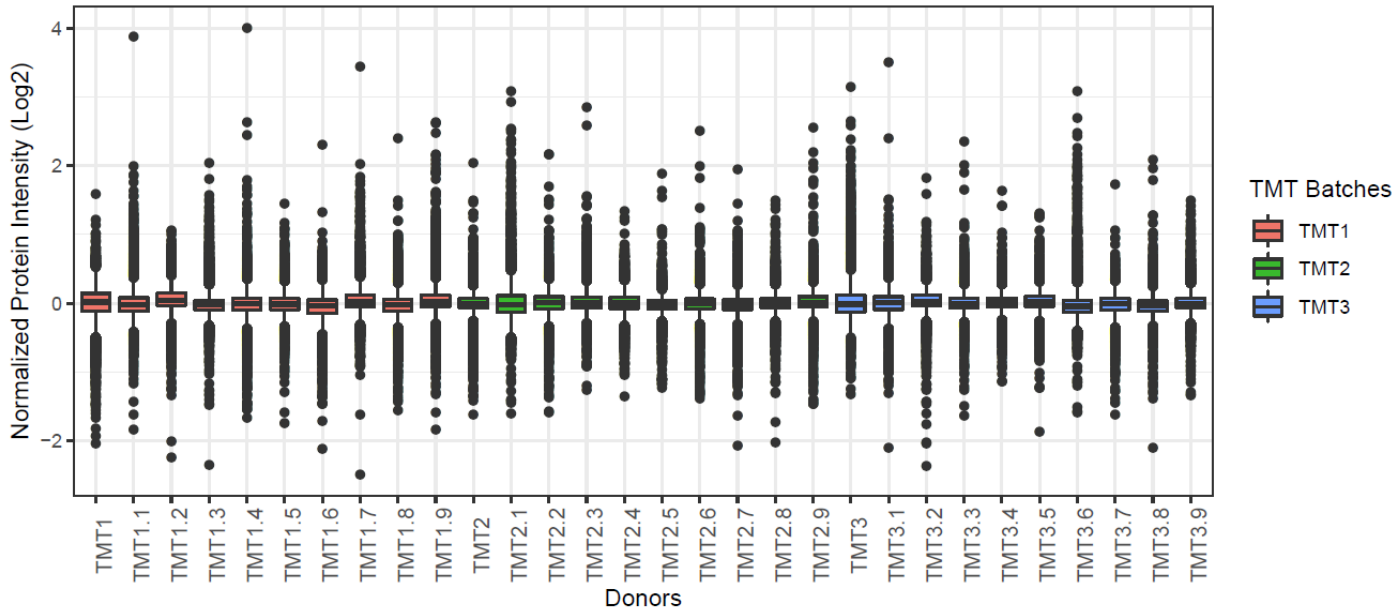

Figure 2-figure supplement 1. Boxplot of all donors from 3 TMT batches. X-axis shows all the donors including repeats and y-axis shows the median normalized log2 protein intensity. Each batch is color coded.

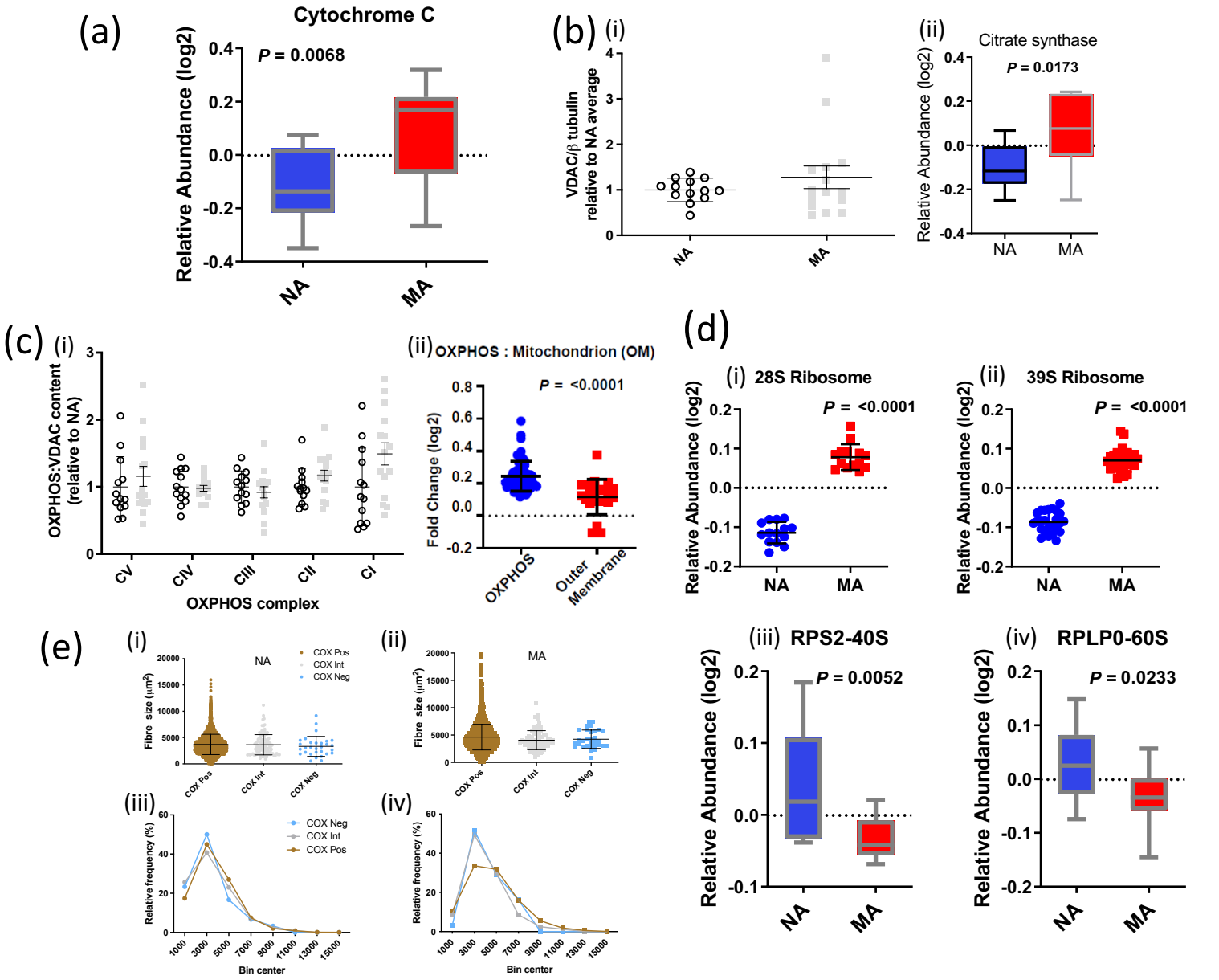

Figure 3-figure supplement 1. Abundance of mitochondrial proteins, VDAC and subunits of the OXPHOS chain assessed by western blot and MS in MA versus NA. (a) Higher abundance of cytochrome C in MA. (b) Abundance of mitochondrial proteins. (i) There was no significant difference in VDAC assessed by Western blot between MA (n=15) and NA (n=13, insufficient tissue form one subject). Removal of the MA outlier made no difference to significance values (Wilcoxon rank-sum). (ii) Citrate synthase protein content by proteomics was higher in MA. (c) (i) There was a significant main effect (p=0.046) indicating higher OXPHOS complexes relative to VDAC in MA (grey squares). Western blot values are expressed relative to NA average (empty circles). Graphs show means and standard deviations. (ii) Consistent with these Western blot analyses, Log2 FC expression of 64 significant OXPHOS complex proteins versus 21 VDAC proteins was higher in MA than NA. (d) Ribosomal proteins. Mitochondrial ribosomes are overrepresented in MA and cytoplasmic ribosomes are underrepresented in MA. (i) Twelve 28S ribosomal proteins were averaged and (ii) twenty-four 39S ribosomes are averaged and shown, respectively. (iii) 40S ribosomal protein RPS2 is significantly lower in MA versus NA, and similarly (ii) the abundance of RPLP0 60S protein was higher in MA. (e) Size distribution of respiratory chain compromised fibres: range of observations in (i) NA and (ii) MA, along with the frequency distributions in (iii) NA and (iv) MA. There was no significant difference in the average fibre size between COX^{POS}, COX^{Int}, or COX^{Neg} cells in either NA or MA subjects and there was no significant increase in the frequency of COX^{Neg} cells in the smallest size bin. Circles are NA and squares are MA, brown symbols are COX^{Pos} fibres, grey symbols are COX^{Int} fibres, blue symbols are COX^{Neg} fibres. Graphs show means and standard deviation.

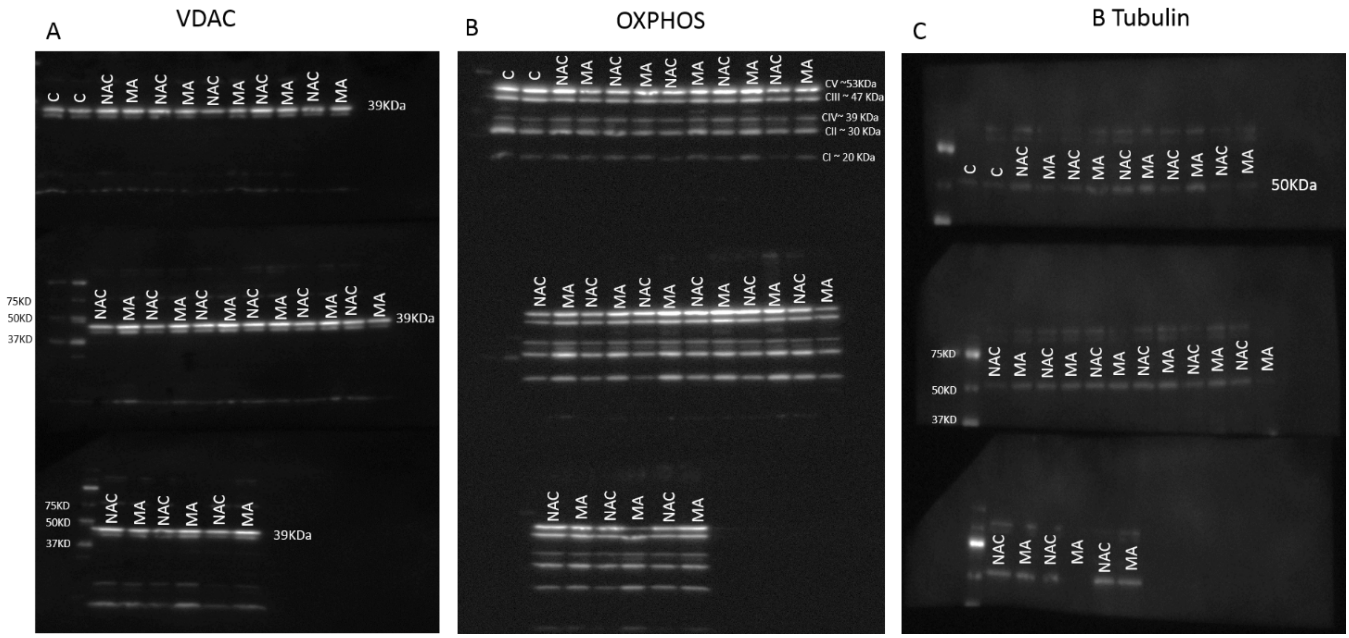

Figure 3-figure supplement 2. Mitochondrial protein quantification. Mitochondrial protein quantification was performed by immunoblotting of the mitochondrial proteins VDAC (**A**) and the components of the OXPHOS system (**B**). The samples were loaded alternatively i.e. one MA and one NA. Gels held 12 samples plus a pre stained protein standard (161-0375 BioRad). Quantification was performed on images taken with all three gels present. The gels were probed for tubulin (**C**), stripped, then probed for VDAC, stripped again and then probed for the OXPHOS subunits. C = samples of protein from subjects not included in this study.

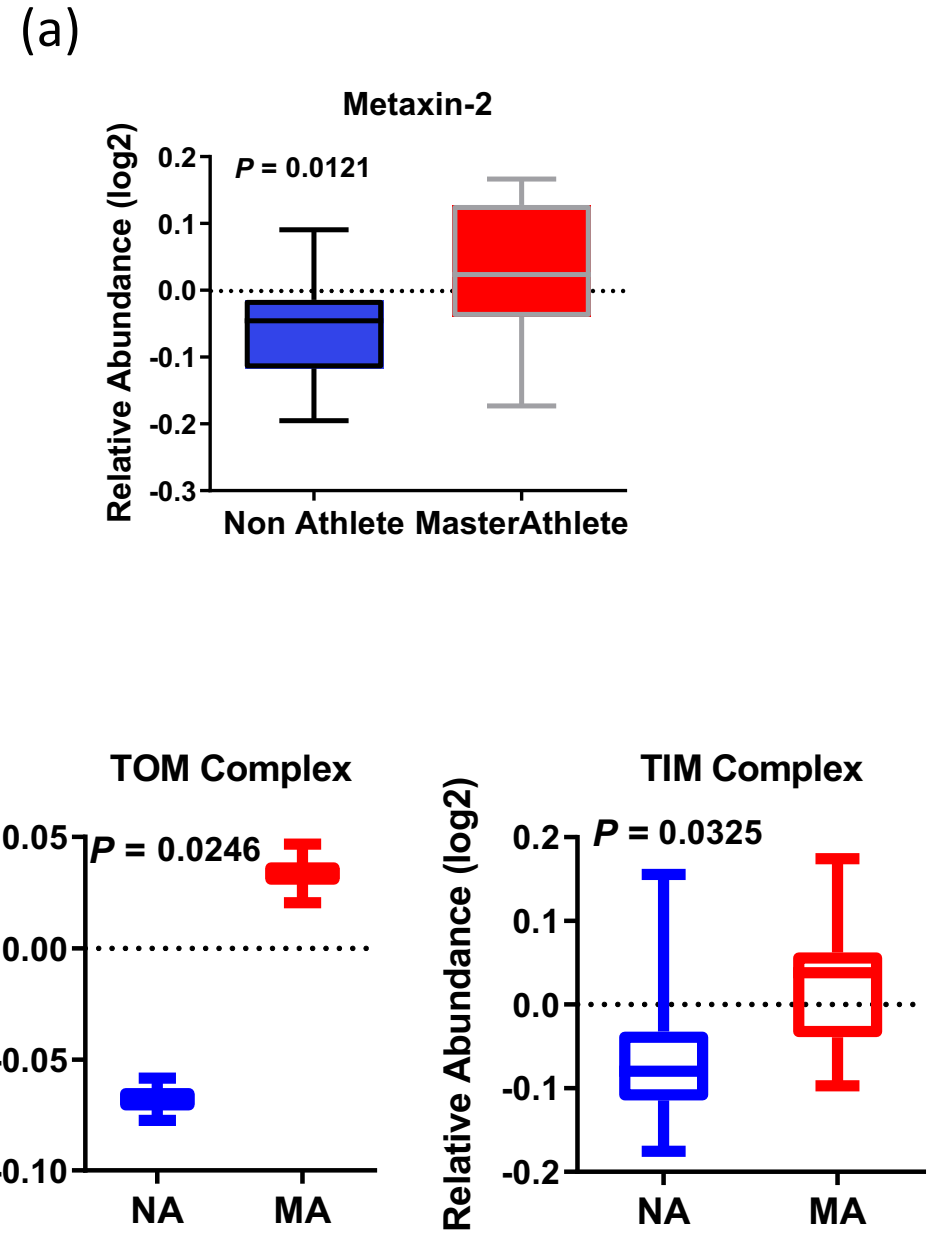

Figure 3-figure supplement 3. mtDNA enrichment analysis and cristae formation. (a) Relative protein abundance of metaxin. (b) TOM complex and TIM complex. The average expression of all the proteins quantified for TOM complex (TOM22 and TOMM40) and 9 TIM complex proteins are on bottom figure panel.

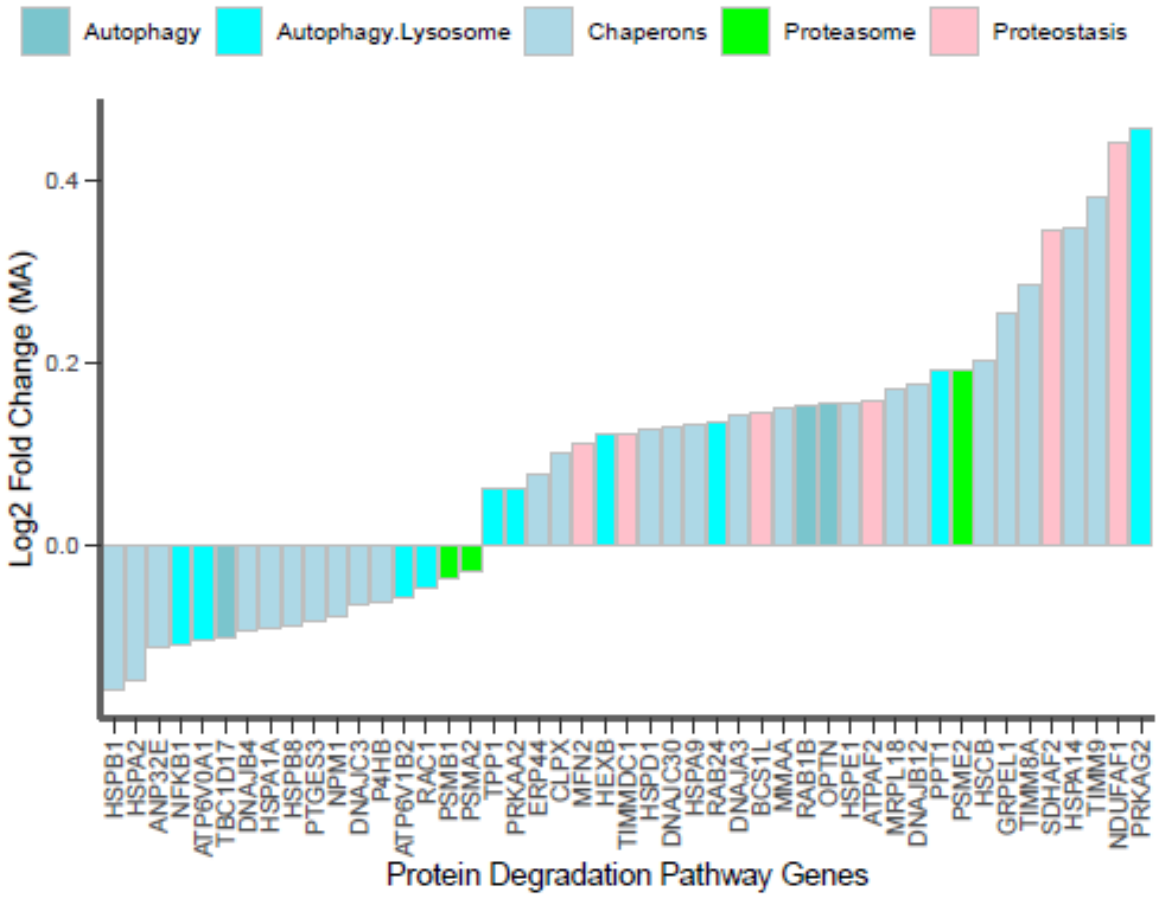

Figure 3-figure supplement 4: Autophagy lysosomal system, and ubiquitin proteasome pathway proteins. Expression of significant proteins from autophagy and proteasome pathways are shown for MA vs NA. Each bar is a protein with the corresponding gene name showing decrease in abundance to increase in abundance (left to right). X-axis is the protein, and Y-axis is the log2 FC of the MA proteins. Different categories of the autophagy, proteostasis proteins are color coded.

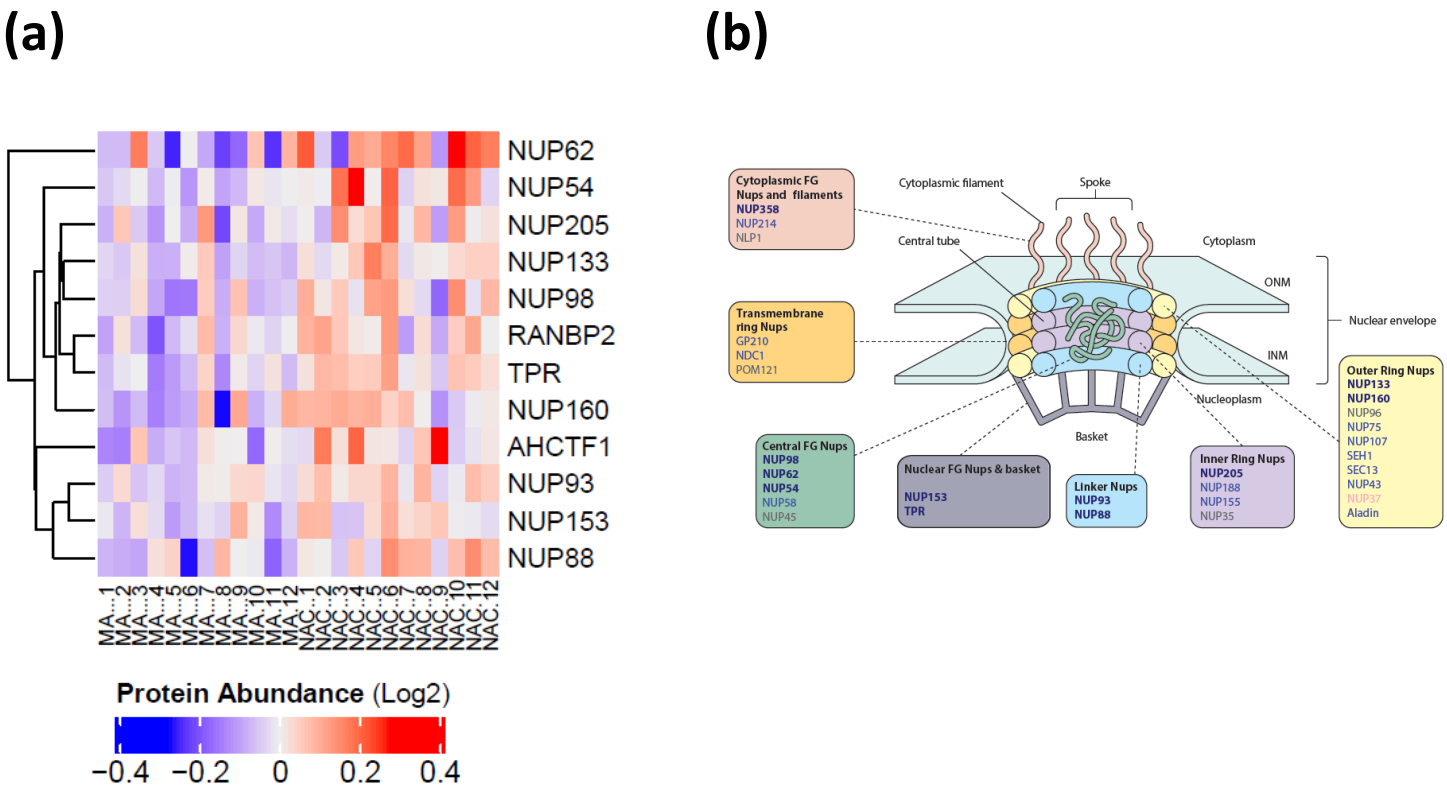

Figure 3-figure supplement 5: (a) Nuclear pore membrane proteins. Expression of significant nuclear pore proteins for all donors. The first 12 columns are MA donors followed by NA, The abundance of protein expression is lower in MA versus NA. (b) Underrepresented MA proteins in the nuclear pore structure. Structure of nuclear pore complex (NPC) and the proteins underrepresented showing significant protein coverage for all classes of NPC. Bold blue gene names are significant underrepresented proteins ($p<0.05$), blue gene names are quantified but not significant ($p>0.05$) and gray gene names are not detected in the dataset.

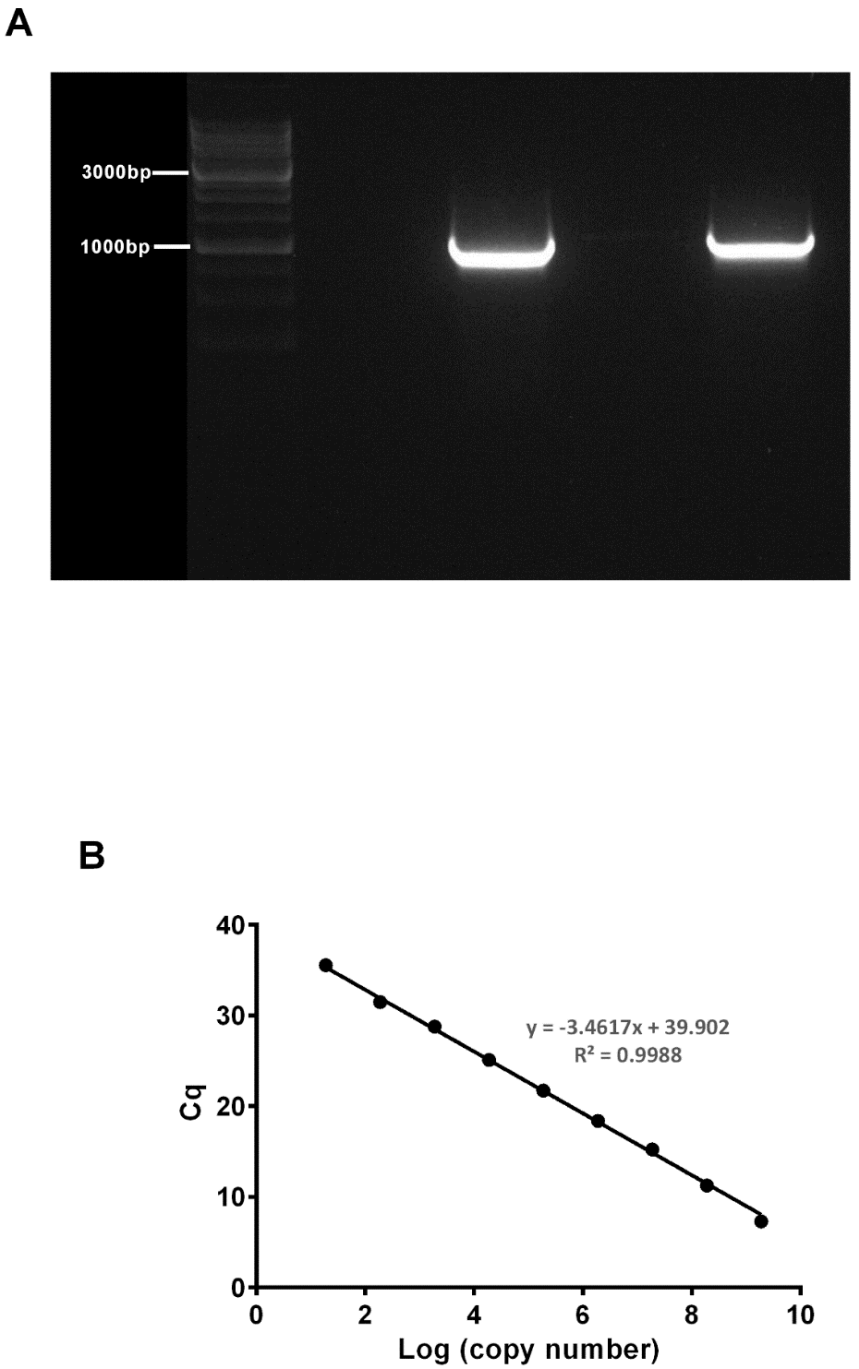

Figure 3-figure supplement 6. Generating a standard curve in order to determine absolute mtDNA copy number. A 1011bp fragment (**A**) containing the MTND1 region was amplified and then run (both visible lanes) with a 25K ladder (Diamed). Following separation on a 1% gel the band was extracted using a QIAquick Gel Extraction Kit (Qiagen) and the product quantified using a spectrophotometer. (**B)** The mtDNA fragment was then serially diluted down to generate a standard curve which was then run on a *MTND1* TaqMan® qPCR assay multiple times to generate a consistent line and equation. All subject samples were run at the same time along with the curve in order that their mtDNA copy number could be determined.

Age Group	**20-34**	**35-49**	**50-64**	**65-79**	**80+**	***P*-value**	**R^2**
	(*n*=13)	(*n*=11)	(*n*=12)	(*n*=12)	(*n*=10)	--	--
Gender	*M*8, *F*5	*M*7, *F*4	*M*7, *F*5	*M*8, *F*4	*M6*, *F4*	--	--
Age (yr)	27.2 ± 3.3	41.3 ± 4.5	57.1 ± 4.7	70.3 ± 2.3	82.4 ± 2.4	--	--
Race	9*C*, 2*AA*, 2*A*	5*C*, 6*AA*	8*C*, 4*AA*	10*C*,1*AA*,1*A*	9*C*,1*AA*	0.0958	--
***BMI, kg/m^2**	25.9 ± 2.8	26.4 ± 2.6	26.6 ± 3.2	26.4 ± 2.4	25.2 ± 3.9	0.3458	0.007
Height (cm)	172 ± 11	177 ± 10	169 ± 4	172 ± 11	172 ± 6	0.3985	--
***Weight (kg)**	76 ± 10	81 ± 9	77 ± 12	75 ± 13	73 ± 16	**1.74E-05**	0.34
Education (yr)	16 ± 3	14 ±3	14 ± 2	16 ± 2	17 ± 2	0.3305	--
***Waist Circumference(cm)**	82 ± 7	87 ± 7	90 ± 11	92 ± 11	92 ± 13	**6.32E-06**	0.39
***KEIS (left) ±**	192 ± 31	208 ±55	200 ± 71	165 ± 62	130 ± 42	**4.29E-07**	0.40
***KEIS (right) ±**	194 ± 38	220 ± 65	194 ±78	169 ± 53	147 ± 57	**2.41E-07**	0.41
†Physical Activity	1.8 ± 1.4	1.8 ± 1.3	2 ± 1.1	2.3 ± 1	1.5 ± 1.1	0.5145	--

Figure 5–figure supplement 1. Baseline characteristics of the GESTALT skeletal muscle participants. The participants are classified into 5 different age groups. Gender: The number of donors is represented in numeric, *M* is Male, *F* is Female. Age in years as mean and standard deviation (SD ±) for each age group. Race: number of donors is shown in left and race is shown in italics, *C* is Caucasian, *AA* is African American, and *A* is Asian. Body Mass Index (BMI) expressed as mean and SD (±) for each group. *P*-value is calculated by 1-way ANOVA with Kruskal-Wallis test.

*****_P_-value calculated from linear regression model, gender adjusted.

± Knee Extension Isokinetic Strength (KEIS) (30^0/sec; Nm).

†Physical activity is calculated from the sum of weight circuit, vigorous exercise, brisk walking and casual walking and summed as high intensity physical activity per week. This is further categorized into 0 (not active),1 (moderately active), 2 (active), and 3 (highly active) and expressed as mean of categorical variables (0,1,2,3) ± SD.